Coordination Chemistry Reviews, 78 (1987) 253–331
Elsevier Science Publishers B.V., Amsterdam – Printed in The Netherlands

Medical Diagnostic Imaging with Complexes of ^{99m}Tc

Michael J. Clarke and Lisa Podbielski

Contents

Introduction.

It is now over twenty-five years since the development of the "technetium generator" revolutionized nuclear medicine by making the radionuclide, ^{99m}Tc, easily available to clinical facilities

0010-8545/87/$27.65

[1]. ^{99m}Tc is presently the most commonly used nuclide for the imaging of internal organs by scintillation cameras and it is estimated that sales of the generator, derivatization kits and related equipment is on the order of $\$10^8$/yr. Since this technology readily lends itself to automation, sophisticated data handling, and graphical presentation of the physiological functions of internal human organs, it is now at the forefront of the clinician's arsenal of safe, informative, diagnostic techniques.

Owing to its position in the middle of the transition elements, technetium exhibits a wide range of chemistry. Medically useful and potentially useful complexes in aqueous solution exist in oxidation states ranging between Tc(I) and Tc(VII), with Tc(III), (IV) and -(V) being somewhat more common. A number of excellent reviews dealing with the chemistry [2 ,3 ,4 ,5 ,6 ,7 ,8 ,9] and structure [10] of technetium compounds have recently been published. Since the initial impetus to the field was supplied by medical diagnosticians, primarily interested in developing easily prepared materials to yield useful organ images, full chemical characterization was rarely performed on diagnostic preparations. It has only been within the last decade that coordination chemists have begun concerted efforts to clarify the structure and chemistry of these radiopharmaceuticals, devise general synthetic methods and employ this information in the design of new imaging agents. This review attempts to correlate the now burgeoning chemistry of technetium (through June, 1985) with the preparation and biodistribution of the clinical agents. After a brief description of commonly used synthetic methods and imaging techniques, technetium radioscintigraphic compounds are surveyed by order of the organs they image.

Chemistry and Instrumentation

Technetium Generation. The radiophysical properties of the nuclide ^{99m}Tc, which exists in a metastable nuclear excited state, are nearly ideal for diagnostic radioscintigraphy. As in all types of photography, precise imaging depends on accurately directing the radiation toward the imaging medium. In radioscintigraphy, collimation of the γ-rays before striking the scintillation medium

is accomplished by an arrangement of hexagonal holes aligned through a thick piece of lead [11]. While highly energetic γ-rays require very thick collimators, the 141 KeV γ-ray from ^{99m}Tc falls in a convenient range handled by a reasonable thickness of lead, but is sufficiently energetic to penetrate through several layers of tissue and give rise to a scintillation event on striking a sodium-iodide crystal.

A typical scan involves 20-30 mCi of ^{99m}Tc, which rapidly decays to the long-lived ^{99}Tc ($t_{1/2}$ = 2.13 x 10^5 yr). The 6.02 hr half-life of ^{99m}Tc allows for the administration of high radiation counts, since the biological dose is relatively small when integrated over the fairly short time it is emitted. The absence of any concomitant α- or β-radiation also represents an advantage over other isotopes and together these features allow for the repetition of diagnostic scans as needed. While a portion of the technetium may remain in body tissues for considerable periods, the daughter isotope, ^{99}Tc, emits only β-radiation with a maximum energy of 292 KeV and, owing to its long half-life, the additional radiation dose from the residual ^{99}Tc is essentially negligible.

The "technetium-generator" contains $[^{99}MoO_4]^{2-}$ adsorbed at the top of a lead-shielded alumina ion-exchange column. The ^{99}Mo decays with a 67 hr half-life by β^--emission to give $[^{99m}TcO_4]^-$. Owing to the difference in charges between the molybdate and pertechnetate ions, only the latter elutes from the column with physiological saline solution (0.15 M NaCl). Since the ^{99m}Tc undergoes further decay to ^{99}Tc, the eluant contains both nuclides. The activity of the eluant and the relative quantities of ^{99m}Tc and ^{99}Tc depend on the age of the column and the period of time since it was previously "milked". Total technetium concentrations in the eluant are variable, but are usually in the range 10^{-8} to 10^{-6} M [12]. The minimum quantity of pure ^{99m}Tc necessary for adequate imaging is on the order of a few nanograms, so that even with several times this amount of ^{99}Tc present, the chemical toxicity is negligible.

Instrumentation. Thick thallium-activated sodium iodide crystals are of sufficiently high density to absorb a significant fraction of γ-radiation below 500 KeV. Absorption of the radiation

results in ejection of a core electron, which imparts its kinetic energy to the crystal matrix. The resulting emission of light photons is directly proportional to the number and energies of the incident γ-rays. The light energy is then converted by a photomultiplier tube or photodiode into an electrical pulse proportional to the amount of light produced, which is then converted into a graphical display. The area monitored by the crystal is inversely proportional to the length of the collimator, while the resolution of the display is directly proportional to it. Imaging thyroids, which are small, easily located organs near the surface is done with a high-resolution collimator focusing on a single, wide crystal. Large organs, such as kidneys, which may vary in location, are best studied through an array of smaller crystals each with relatively short collimator [13].

Rectilinear scanners use large NaI(Tl) crystals 2 inches thick and 3-8 inches in diameter with focused collimators, which may be changed to focus at different depths within the body. The detector is moved in a back-and-forth rectilinear raster path over the area of interest to produce the desired image (see Figure 1). Dual or quadruple detector heads may be employed to decrease scanning time and Anger-type scintillation cameras (see below) employing crystal arrays have been developed. The electrical pulse from the photodetectors is fed to a graphical display device or a cathode ray tube to expose x-ray film for a permanent record.

Anger cameras are now used to perform most of the high-resolution and rapid-scan studies in nuclear medicine. These consist of an array of NaI(Tl) detectors, each having a single-hole collimator. This array is sufficiently wide to cover the width of the body and moving the array from head to toe provides a whole-body scan. Intensity data is recorded according to the position of

Fig. 1 (SEE OPPOSITE)

A Schematic diagram of a simple rectilinear scanner showing raster scan. The detector output moderates a beam of light, whose movement is synchronized with that of the detector and paints the image onto photographic film.

B An array of 5 detectors each of which focuses on a narrow rectangular area. By producing a 5 line scan in alternating directions with each pass, less time is required to complete the image.

Scintigraphic Scanners

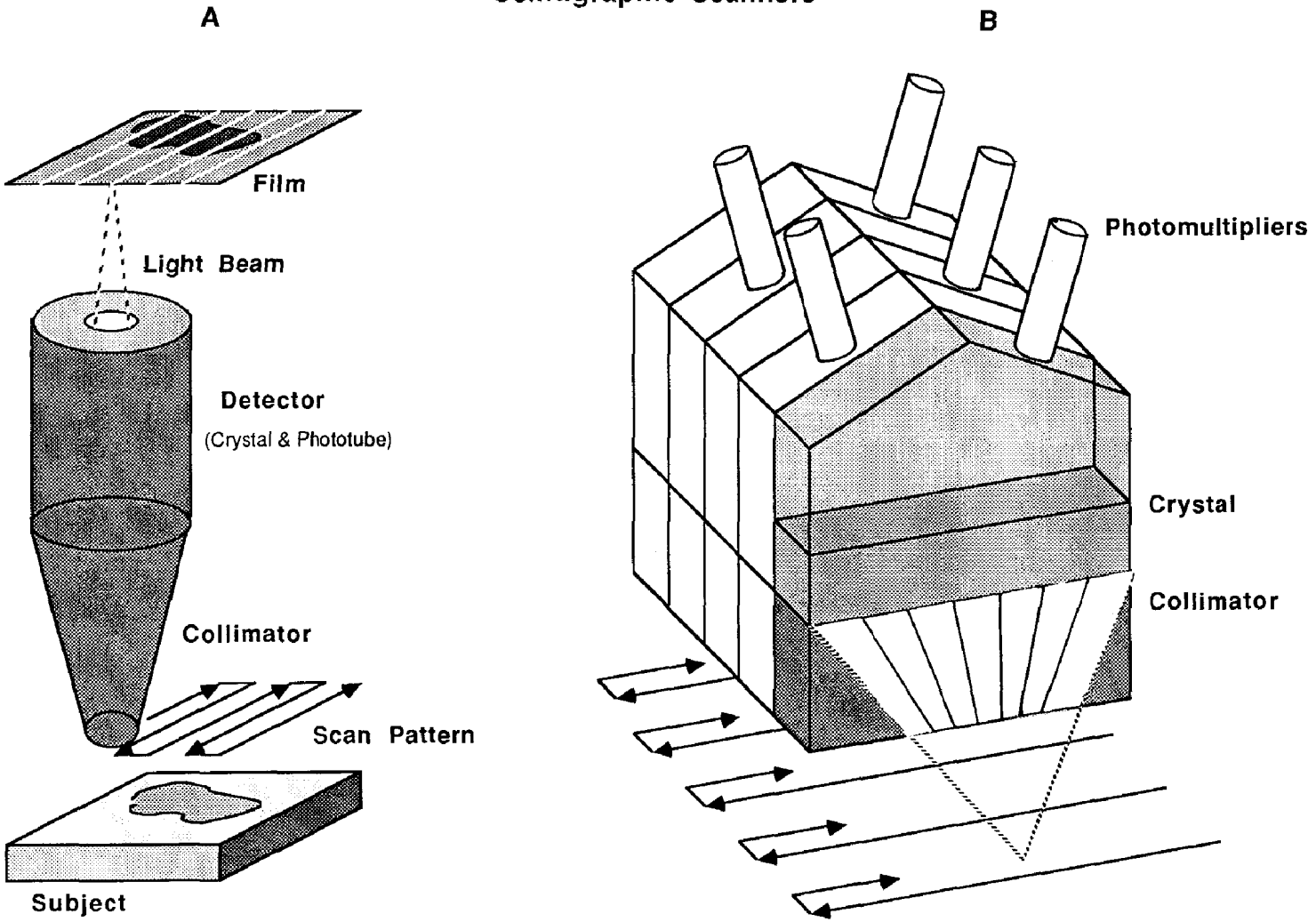

the detector in the array and the position of the moving array, so that a complete two-dimensional picture results. The integrated data are displayed directly on an oscilloscope or stored in digital form.

Cameras consisting of a rectangular array of small area NaI(Tl) crystals each connected by light pipes to two photon counting devices (one for the row and column of the detector in the array) offer higher resolution and more rapid acquisition times by virtue of the parallel processing simultaneous events [14]. A relatively recent instrument utilizes a mosaic array of over 2,500 CsI(Tl) crystals layered on an image intensifier consisting of a photocathode face, which emits electrons upon exposure to scintillation events. The electrons are accelerated and focused before striking a phosphor screen, which is then photographed. Direct transduction of the emitted photon to an electrical pulse is possible with Si, Ge(Li), or CdTe semiconductor detectors, which efficiently discriminate against scattered photons and background events by providing better energy and spatial resolution.

Single photon emission computed tomographic (SPECT) scanners, which generate sectional slices of the variation in radioactivity throughout the body, are now available. Imaging selected planes within the subject makes lesions more obvious, separates them from the radioactivity of superficial structures, and gives information about their depth [11,15]. The resolution and sensitivity of the method is highly dependent on the design of the collimators and the geometry of the detector array. However, for areas, such as the head, which can be easily surrounded by the detector array, ^{99m}Tc-SPECT has the potential for providing the high resolution rapid scanning necessary in handling trauma cases and for visualizing abnormalities in blood flow to the brain.

Synthetic Methods. Since ^{99m}Tc is supplied from the technetium generator as aqueous $[^{99m}TcO_4]^-$, all synthetic methods used in nuclear medicine must begin with this tetrahedral, d^0 ion. The concentrations of $[TcO_4]^-$ available may be as high as the micromolar range, so that syntheses developed with milligrams of starting material are potentially transferrable to the clinical setting [12]. Most chemical characterization is carried out on

compounds prepared with milligram quantities of the much more stable ^{99}Tc.

The energy of the β-rays emmitted by ^{99}Tc are almost twice as energetic as those from ^{14}C (156 KeV) but less so than ^{32}P (1,710 KeV), which are both commonly handled (in smaller amounts) in normal biochemistry laboratories. The β-emission from milligram quantities of ^{99}Tc is effectively stopped by solutions and normal laboratory glassware, and the soft x-ray radiation (Bremsstrahlung) resulting from stopping the β-ray is not a significant problem. The specific activity of ^{99}Tc is 17 mCi/g. Assumming the handling of 100 mg quantities of the commercially available $NH_4[TcO_4]$ [16], most university licenses would require only that the work be done on a disposable surface in a marked hood with appropriate protective clothing, a personal dose meter and geiger counter. In addition, the handling of gram quantities generally necessitates a restricted single-use area, lucite shielding, periodic radiation surveys and a check of the user after operations. With the exception of the lucite shielding, it is the author's opinion that the more stringent requirements should always be followed, with particular care taken to prevent possible ingestion, which may unsuspectedly arise from vapors or small air-borne particles containing ^{99}Tc. Finally, owing to the long half-life of ^{99}Tc, any surface not easily freed of radioactivity will always remain contaminated. Syntheses and animal studies using ^{99m}Tc require a minimum of the stricter requirements and significant lead shielding.

Any synthetic procedure expected to be useful in a clinical setting must fulfill fairly constringent requisites. The synthesis must start from 10^{-8} to 10^{-6} M solutions of $[TcO_4]^-$ in physiological saline. The reagents and the injectable product must be sterile and nontoxic. Since side products generally interfere with the desired image, the reaction should yield a radiochemically pure product. Owing to the short half life, the synthesis must be complete within a few hours. Moreover, since the procedure is usually carried out by nuclear medical technologists with relatively little training in chemistry, using transfer and reaction vessels surrounded with heavy lead shielding, the synthesis should be extraordinarily simple.[5]

Most ^{99m}Tc-radioscintigraphic agents employ reduced oxidation states; however, the pertechnetate ion itself has been used for brain and thyroid imaging. In the absence of reducing agents, pertechnetate ion is quite stable in aqueous solution. While it can add halides and some nitrogen ligands [17 '18 ,19 ,20 ,21 ,22] to form complexes such as [ClO_3Tc] and [$O_3Cl(bipy)Tc$], it usually binds only through electrostatic interactions. In general, coordination is accomplished upon reduction of pertechnetate in the presence of a good complexing agent. Unreacted pertechnetate often persists in radioscintigraphic preparations and in the presence of oxygen can also result from autoradiation-induced decomposition of ^{99m}Tc-radiopharmaceuticals [23]. The brown-black, insoluble Tc_2S_7 can be precipitated from acidic pertechnetate solutions by H_2S, but is often contaminated with elementary sulfur [24]. In colloidal form Tc_2S_7 is used for imaging the reticuloendothilial system.

Attaining Lower Tc Oxidation States. Pertechnetate is a relatively mild oxidant (E^o = 0.738 V) and is initially reduced by a single-electron step to $[TcO_4]^{2-}$ [25 ,26 ,27 ,28]. In the absence of high acid concentration or good complexing agents, a hydrated, insoluble oxide, $TcO_2 \cdot xH_2O$, is rapidly formed and this "thermodynamic sink" is a nemesis in the development of synthetic methods for desireable new technetium compounds in aqueous solution. Srivastava and Richards have recently discussed the relative merits of a variety of reductants that have been prominently used in the synthesis of technetium complexes [8,29].

Simplified reagent "kits", which involve injecting the generator eluant into a sterile reaction vial containing the reductant and complexing agent, are normally employed in the clinical setting. Tin(II) compounds or electrochemically generated Sn^{2+} have proven to be the most reliable reductants in these convenient commercial reactors [8]. The choice of a reductant can be difficult, since it must react rapidly and completely and not interfere with the biodistribution of the resulting technetium complex. Many organic reductants tend to work slowly or only at high pH, which promotes hydrolysis of reduced technetium species and the formation of TcO_2 [8]. Metal ions have the advantage of being fairly rapid reductants, but have been known to be incorporated into the radiopharmaceutical or hydrolyze, precipitate

and thereby trap some of the ^{99m}Tc, making it unsuitable for the desired imaging procedure. It has been suggested that Sn(II) can affect biodistribution [30] by enhancing the binding of some technetium complexes to liver or kidney enzymes [31] and possibly alter membrane permeability in kidneys [32]. The molecular structure of $[Tc(DMG)_3SnCl_3(OH)]\cdot 3H_2O$ (DMG = dimethylglyoxime) clearly shows that Sn(II) can be incorporated into technetium complexes prepared by stannous reduction of $[TcO_4]^-$ [33].

Deutsch has recently pointed out that the most likely kinetic situation in the formation of radiopharmaceuticals from pre-prepared "kits" is that the other reactants are present in sufficient excess so that the reaction is pseudo-first order in the metal ion. As a result, the time taken for the reaction to be essentially complete is a function only of the pseudo-first order rate constant and not of the metal ion concentration. In this case, chemistry developed with larger-scale quantities of ^{99}Tc is directly applicable to ^{99m}Tc radiopharmaceuticals. The same is true for the less-likely case of zero-order kinetics; however, when second or higher order kinetics hold, the half-life of the reaction is inversely proportional to the technetium concentration. In these instances, the desired reaction may proceed too slowly with respect to the half life of the nuclide or other undesireable first-order reactions. Conversely, if the second-order reaction is undesireable, it may decrease the yield of the imaging agent when significant amounts of ^{99}Tc are present in the generator eluant to increase the total technetium concentration [5].

With the exception of the Tc(VI)-nitrido complexes (see below), the Tc(VI) oxidation state is generally unstable in water. A stable, trigonal prismatic complex, $[(C_6H_4NHS)_3Tc]$, has been described; however, its EPR spectrum indicates the odd electron to be localized mainly on the ligand [34 ,35]. Oxo Tc(VI) species, such as $[OCl_5Tc]^-$, can be prepared by the reduction of $[TcO_4]^-$ with H_2SO_4/HCl, $SOCl_2$ or $POCl_3$ and exhibit strongly coupled EPR spectra with pronounced spin-orbit coupling, when stabilized in acidic media [36].

The initial reduction of $[TcO_4]^-$ more commonly proceeds by two electrons to yield oxotechnetium(V) ions. This can occur through

oxygen atom transfer to a reductant such as a stannous complex, a phosphine or an arsine. The preparation of the technetium(I) complex, $[(MeO)_3P)_6Tc]^+$, by heating excess $P(OMe)_3$ in a methanolic solution with $Na[TcO_4]$ demonstrates the powerful reductive action of trimethylphosphite on an oxo species [37]. In a Tc(V)/Tc(III) system employing $[OCl_2(HBpyz_3)Tc]$ (where $HBpyz_3$ = hydrotris(1-pyrazolyl)borate) and triphenylphosphine the complex $[OCl_2(Ph_3PO)(HBpyz_3)Tc]$ was isolated as an intermediate, with the triphenylphosphito ligand being easily displaced by Ph_3P or pyridine [38]. Since in attaining Tc(V) from Tc(VII) a maximum of one oxygen atom can be displaced by oxo transfer to the reductant, the other oxygens must be removed by proton addition to form water. In the reaction of $[TcO_4]^-$ or no carrier added $[^{99m}TcO_4]^-$ with cold, concentrated HCl a yellow species thought to be *fac*-$[O_3Cl_3Tc]^{2-}$ is initially formed, which then rapidly oxidizes chloride to produce chlorine and the green, $[OCl_4Tc^V]^-$ [2,39]. This complex [40 ,41] and the bromo [42] and iodo [43] analogs represent useful synthetic starting materials even at the carrier-free level. At neutral pH they all undergo rapid hydrolysis and disproportionation to give $[TcO_4]^-$ and TcO_2.

Chemistry of Lower Valent States. Several coordination geometries have been observed with Tc(III), Tc(IV) and Tc(V). In the Tc(V) oxidation state mono- and dioxo-ions are prominent in aqueous media. In general the $[Tc{=}O]^{3+}$ core is present in complexes containing π-donor ligands in the equatorial plane, while the *trans*-dioxotechnetium(V) moiety obtains with π-acceptor ligands or ligands that do not form π-bonds [2,6,9,10]. A number of square-pyramidal compounds are now known with apical oxygens and halide, sulfur or oxygen equatorial ligands (see Figure 2) [44]. These complexes exhibit fairly short Tc-O bond distances (with an average of 1.65 Å) indicating at least partial triple bonding involving the d_π-orbitals. Such monopolization of metal bonding orbitals produces a pronounced *trans*-effect. Nitrogen and oxygen chelating groups may force coordination opposite an oxo ligand with a resulting distorted geometry in which the ligand *trans* to the oxo exhibits a lengthened bond to the technetium [45]. Coordination of water, chloride [46] and alcoholate [47] groups have also been observed *trans* to the oxo, and their ability to function as π-donors may diminish the oxo *trans*-effect. Partly as a result of π-

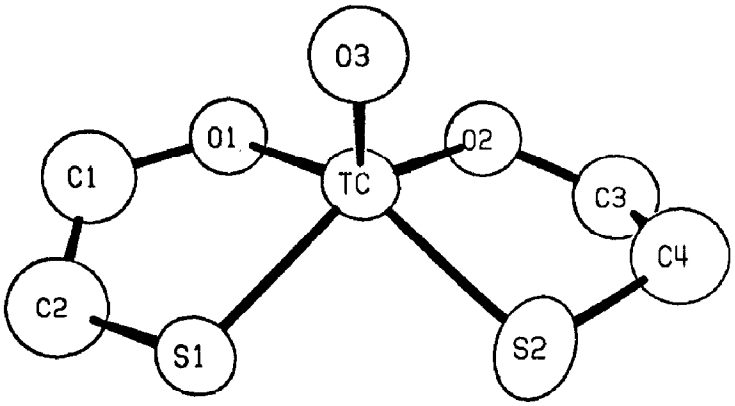

Fig. 2 Structure of bis(2-mercaptoethanolato)oxotechnetate [44].

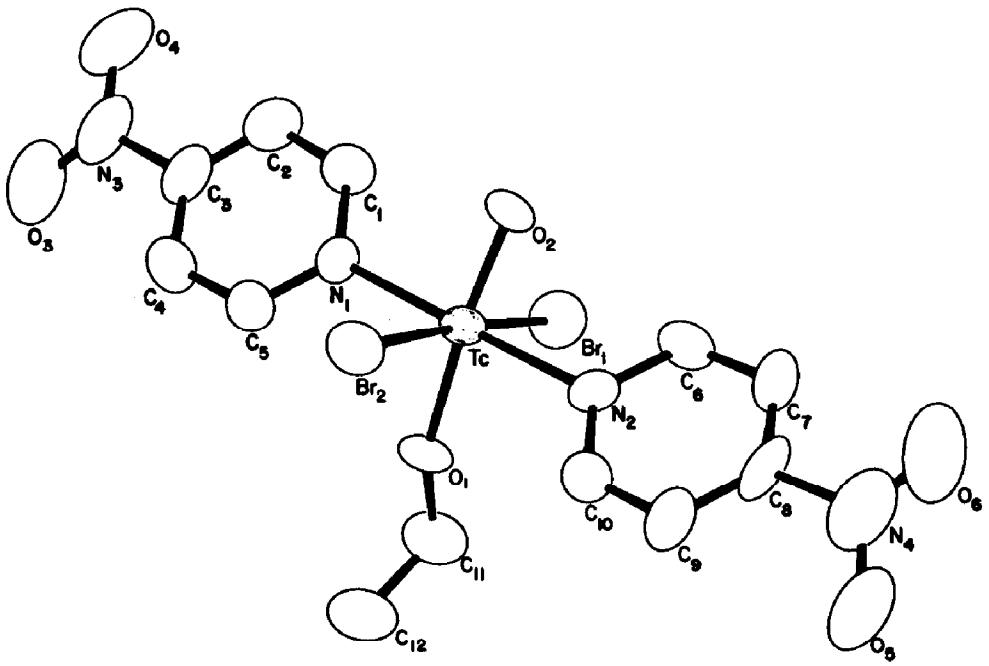

Fig. 3 Structure of af-dibromo-b-ethoxo-d-oxo-ce-bis(4-nitropyridine) technetium(V) [47].

interactions, water or alcohol molecules added at the *trans*-position are easily deprotonated to hydroxide or alcoholates (see Figure 3) [46]. Hydroxide most frequently undergoes a second deprotonation to yield the oxo ligand. The equilibrium constant for adding a chloride *trans* to the oxo in $[OCl_4Tc]^-$ is 0.6 and EXAFS studies reveal that this is held at a slightly longer bond distance (2.50 Å) than the *cis* chlorides (2.36 Å) [48].

Complexes with mono- and bidentate nitrogen and oxygen ligands are usually nominally octahedral with the oxygens opposite one another at a typical Tc=O bond distance of 1.75 Å (see Figure 4)[49 ,50 ,51 ,52]. The $[Tc{=}O]^{3+}$ and $[O{=}Tc{=}O]^{+}$ cores are readily distinguished on the basis of their infrared stretching frequencies, which occur at 930-1020 cm^{-1} for the former and 790-860 cm^{-1} for the latter. Owing to a strong tetragonal distortion of the ligand field exerted by the oxo group, these compounds are usually diamagnetic with the two d-electrons being paired in the d_{xy} orbital. When no steric or *trans*-effects are operating, the average Tc(V)-N single bond distance is 2.15 Å. By analogy to a structurally characterized rhenium analog [53], a binuclear complex with diethyldithiocarbamate is thought to contain a linear $[O{=}Tc{-}O{-}Tc{=}O]^{4+}$ core [2,54].

Nitrido complexes bearing structural analogies to the oxo species have also been reported [55 ,56]. The strong π-acceptor properties of the nitride appear to promote the binding of relatively "soft" ligands such as dithiocarbamates and phosphines. The compounds are usually prepared by hydrazine reduction of $[TcO_4]^-$ in dilute HCl followed by addition of the phosphine ligand after adjusting to neutral pH. This versatile method provides for series of complexes in which characteristics such as lipophilicity can be systematically varied [57]. Interestingly the use of formamidinesulphinic acid as the reductant in the presence of $Na[S_2CNEt_2]$ results in the carbonyl complex $[(CO)(Et_2NCS_2)_3Tc]$. The Tc≡N bond lengths are normally around 1.61 Å and the Tc≡N stretching frequencies in the range 1000-1110 cm^{-1} [58]. Similar to the complexes with the $[O{=}Tc]^{+}$ core, nitrido complexes can accept a ligand *trans* to the nitride under suitable conditions [59].

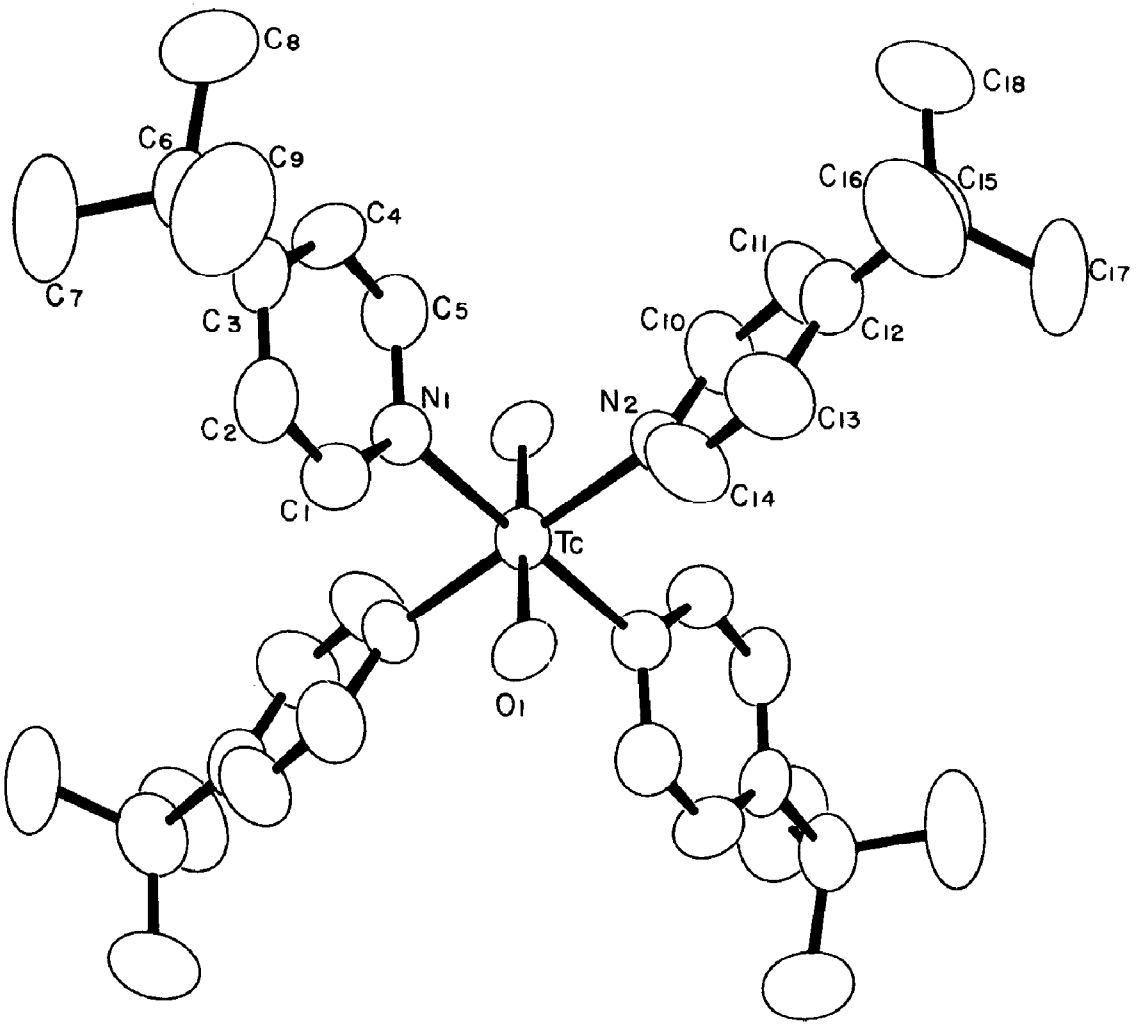

Fig. 4 Structure of **trans**-$[O_2(TBP)_4Tc(V)]^+$ (TBP = 4-**tert**-butylpyridine) [51].

The Tc≡N bond is sufficiently strong that it survives oxidation to Tc(VI) and even Tc(VII). The complex $[NBr_4Tc]^-$ is readily prepared from $[TcO_4]^-$ and sodium azide in HBr and along with the corresponding chloro species promises to be a useful starting material for the synthesis of Tc(VI)-nitrido complexes. These complexes exhibit ideal C_{4v} symmetry with average Tc≡N distances of 1.588 Å. The EPR spectra of nitrido Tc(VI) complexes exhibit strong coupling to the ^{99}Tc nucleus and pronounced spin-orbit coupling [60]. The reaction of either disulfur dichloride or thionyl chloride with $[N(Et_2NCS_2)_2Tc]$ yields a seven-coordinate thionitrosyl Tc(III) complex, $[(SN)Cl_2(Et_2NCS_2)_2Tc]$. Structural analysis shows linear Tc=N=S bonding with a Tc=N distance of 1.75 Å and a N=S bond length of 1.52 Å, indicating that the thionitrosyl group is a three-electron donor with a formal positive charge[61].

Relatively few mechanistic studies on the formation of technetium complexes have been carried out; however, the kinetics of substituting 1,2-dithiols onto $[OCl_4Tc]^-$ and the analogous catecholato and ethyleneglycolato complexes in methanol demonstrate that the mechanism and the final products of these reactions are quite sensitive to the structure of the incoming ligand [62]. Addition of the dithiolate to the catecholato complex involves a monomeric intermediate apparently containing one sulfur ligand, while reactions with the ethyleneglycolato species proceed to the final product, $[O(SCH_2CH_2S)_2Tc]^-$, apparently without formation of an intermediate.

Substitution onto the tetrachloro complex proceeds through a noncentrosymmetric binuclear complex, $[(TcO)_2(SCH_2CH_2S)_3]$, in which both oxotechnetium ions are square pyramidal, but are canted relative to one another by almost 90^o. One Tc is chelated by a single dithiolate and is bridged by the sulfurs of two other dithiolates to the second Tc, which also holds the two remaining sulfur atoms [63]. Use of an acetamidomethyl-protected 1,2-ethandithiol or 1,3-propanedithiol in methanol resulted in cessation of the reaction once the binuclear intermediate was formed, suggesting that steric hindrance prevents the approach of this ligand to the open sixth position at either Tc. Conversely, 3,4-toluenedithiol reacted directly to yield the monomer $[O(CH_3C_6H_3S_2)_2Tc]^-$.

Formation of the complex *trans*-$[O_2(cyclam)Tc]^+$[64 ,65] (where cyclam = 1,4,8,11-tetraazocyclotetradecane) proceeds with surprising speed considering that the technetium must be inserted into a macrocyclic ligand [66]. One possible mechanism which would account for this is that the reaction proceeds through an intermediate involving $[Tc{=}O]^{3+}$ or $[O{=}Tc{-}OH_2]^{3+}$. Since all the oxo-Tc(V) cores are spin-paired d^2 ions, there is minimal crystal field activation energy to equatorial substitution [5]. Either intermediate would allow initial attack at the position *trans* to the oxo, which would then place the nitrogens in a favorable position to sequentially substitute for each of the equatorial ligands. Owing to the *trans* effect of the oxo, the initially attached nitrogen would soon be labilized and reattach in an equatorial position. Finally, conversion to the *trans*-[O=Tc=O] core is easily effected by water addition at the site *trans* to the oxo followed by rapid deprotonation to a second oxo ligand.

At least partly owing to the crystal field stabilization energy accruing to d^3 ions, Tc(IV) complexes are most commonly octahedral. Their effective magnetic moments are generally in the range expected on a spin-only basis, between 3.6 and 4.1β [6,9]. Complexes with halides or pseudo halides are raidly hydrolyzed to TcO_2 in water unless stabilized by strong acids. With the exception of the thiocyanide complex, single-electron reduction usually results in the ligand loss [67 ,68 ,69 ,70 ,71].

Technetium(III) is a readily accessible oxidation state and has been shown to complex with a variety of ligands in several coordination geometries. In general, Tc(III) appears to require the presence of good π-acceptor ligands such as carbon monoxide or triphenylphosphines for stabilization. The octahedral compound *mer*-$[Cl_3(Me_2PhP)Tc]$ (where Me = methyl and Ph = phenyl) is possible through the reaction of $(NH_4)_2[TcCl_6]$ with dimethylphenylphosphine in absolute ethanol [72]. Carbon monoxide reacts with this compound in refluxing ethanol to give $[Cl_3(CO)(PMe_2Ph)_3Tc]$, a seven coordinate, capped-octahedral complex with C_{3v} symmetry [73]. This compound has the carbonyl residing in the center of the three phosphine groups to form the capped octahedral face and the chlorides comprising the uncapped face. The metal-ligand bond lengths are: Tc-C, 1.86 A; Tc-P, 2.44 A and Tc-Cl 2.48 A.

The structure of *trans*-$[Cl_2(diars)_2Tc]^+$ (where diars = o-phenylenebis(dimethylarsine)) is representative of a class of Tc(III) complexes with diphosphine and diarsine ligands. In this compound the technetium ion exhibits ideal D_{2h} symmetry with a mean Tc-As distance of 2.512 A and an average Tc-Cl length of 2.322 A[74 ,75]. A dinitrogen complex, $[N_2(Diphos)_2Tc(III)]$, has been made from $[Cl_4(diphos)_2Tc]$ by reduction with 2% sodium amalgam in benzene under nitrogen [76].

The hexakisthiourea complex decomposes in water but is stable in alcohol and has proven to be a useful synthetic starting material. It is easily made from thiourea and $[O_4Tc]^-$ in HCl/ethanol or HBF_4/ethanol. A structure determination of $[Tc(SC(NH_2)_6]Cl_3 \cdot 4H_2O$ yielded an average Tc-S bond distance of 2.43 A. The compounds $[Cl_2(diphos)_2Tc]Cl$, (where diphos = bis(diphenylphosphine)ethane), a hexakis isocyanide complex, $[_6(_3(CH_3)CNC)Tc]PF_6$, and a hexakis trimethylphosphite species, $[_6(_3(CH_3O)P)Tc]PF_6$, have been prepared from the thiourea complex by refluxing in methanol with the appropriate ligand [77]. Complexes with analogs of the type, Ph-C=O-CH-C=S-Ph, have also been readily synthesized from the thiourea species [78].

Organ Imaging with ^{99m}Tc Radiopharmaceuticals.

A wide variety of technetium compounds are used to image various organs. Unlike NMR, CAT scanning or ultrasonic imaging, which are often superior for the delineation of anatomic detail, radioscintigraphy reveals not only the structure of the organ but also aspects of its physiological function. Computer manipulation provides for a convenient, reproducible method of background correction, the extraction of quantitative data, and a graphic display of the results. This visualization of the metabolism or clearance of a radiopharmaceutical in real time quickly provides the clinician with clear evidence of the ability of the organ to carry out its function. Selective ^{99m}Tc-imaging radiopharmaceuticals tend to fall into four broad categories: 1) agents which localize in particular tissues by virtue of their properties as transition metal complexes, 2) proteins or macromolecules on which the ^{99m}Tc-label represents a minor perturbation so that they accumulate in organs according to the biological distribution of the macromolecule, 3) ^{99m}Tc-tagged

colloidal particles, which (depending on their size) are removed by the lymph nodes, the reticuloendothelial system (liver, spleen and bone marrow) or trapped in blood capillaries, 4) whole blood cells incorporated with ^{99m}Tc, which are used for vascular, cardiac and hematological studies.

Renal Imaging. Currently several good renal-imaging agents are available for both anatomical and functional studies of the kidney. The performance of the kidney depends upon its ability to carry out its three interelated excretory, regulatory and endocrine functions. While the anatomical structure of the kidney can be determined in significant detail using x-rays, computer assisted x-ray tomography (CAT scans) or ultrasound, it's excretory function is most easily assessed by radioscintigraphy. Since the elimination of small ionic radioscintigraphic agents from the blood is readily monitored by sequential camera images, computer assisted processing of dynamic renal function images provides direct information on the renal blood flow, the glomerular filtration rate, and assessment of the functional renal mass. Quantitation of these paramaters yields valuable diagnostic aids, which can be particularly valuable in evaluating kidney transplants [79].

In designing new radiopharmaceuticals for kidney imaging it is important to aim for rapid and homogeneous distribution throughout the kidney before significant accumulation occurs in the ureters and the lower part of the kidney. This provides for better contrast in visualizing the organ so as to yield detailed information concerning the integrity of the renal parenchyma (function cells as opposed to support tissue). A significant problem encountered is the existence of different excretory pathways, each of which may have several components. While larger, more lipophilic compounds are preferentially removed by the liver, smaller, more polar compounds are apt to be eliminated by the kidneys, and many compounds are eliminated by both. The ideal agent should be eliminated by the kidneys alone.

The kidney nephrons are responsible for filtering small compounds from larger proteins, reabsorbing water and other necessary components and finally secreting the waste products. The first of these processes involves ultrafiltration of the blood in

the glomerulus. This process can be quantitated by measuring the rate of renal clearance of a freely filterable substance, which is physiologically inert and neither secreted nor absorbed by the renal tubules. Tubular secretion can proceed by both active and passive mechanisms, the former having a definite limit on its capacity and the latter being dependent only on the blood concentration or potential gradient across the tubule. For example, many organic acids and bases are actively secreted by the proximal tubules and may also undergo some passive tubular reabsorption dependent on their pK_a's, lipid solubility, and pH of the tubular fluid [78]. The renal tubules possess heavy metal binding sites involving thiol or disulfide groups. As a result, radiopharmaceutical binding at these sites can provide a good picture of the morphology of the organ.

The renogram, which consists of a plot of radioactivity localized within the kidney as a function of time, is a useful tool in assessing renal function. A typical renogram employs a bolus injection of the radiopharmaceutical with sequential images of the kidneys taken every minute for 30-60 min, depending upon how rapidly the agent is excreted. In cases of deteriorating renal function comparison of individual renograms will provide an assessment of the relative performance of each kidney. The amount of activity (above background) accumulated by each kidney (while the amount of radioactivity in the blood is relatively stable but before it has accumulated significantly in the lower collecting system) divided by the sum of activity in both kidneys is the amount of function contributed by that kidney. If the abnormal kidney retains at least 10-25% of the function or if its contribution is essential to keep the patient off dialysis, then restorative surgery, rather than a nephrectomy is indicated [80].

Another measure of kidney performance is the "effective renal plasma flow" (ERPF), which is defined as the product of the renal plasma flow times the extraction efficiency and is taken to be the area under the activity *versus* time curve for one minute beginning at a specified time after injection dependent on the radiopharmaceutical used. The time taken to reach maximal activity within the kidney and to complete excretion of the agent (or the half-time for this process) varies with the imaging agent, but

should be similar for both kidneys. If the agent is eliminated essentially by glomerular filtration alone, then similar parameters are used to define the glomerular filtration rate (GFR) of the kidneys. A recent measure uses the percent of the total administered dose of radioactivity that appears in the kidneys at a specified interval after the injection [81]. With the exception of acute renal obstruction, which is immediately evident from the renal scans, none of these parameters alone constitutes a diagnostic basis for a specific renal disease.

Since pertechnetate ion is effectively reabsorbed by the tubules, it cannot be used measure the glomerular filtration rate; however, it has been extensively used to determine blood flow to the kidneys. The first technetium radiopharmaceutical with reasonably good kidney specificity was a mixture in which pertechnetate was reduced with ascorbate catalyzed by iron [82]. A variety of sugars (mannitol, inulin, sorbitol [83]), hydroxylated carboxylic acids (gluconate [84], mannonate, citrate [85], glucoheptonate [86]) and chelating agents (EDTA [87], DTPA [88 ,89 ,90], dimercaptosuccinic acid (DMSA) [91], penicillamine [92 ,93], dimercaptopropanesulphonate [94 ,95], and N,N′-bis(mercaptoacetamido)ethylenediamine [96 ,97 ,98 ,99], have since been shown to have utility for renal scans. Few of these have been well characterized and some are mixtures of several ^{99m}Tc-complexes; however, structural data is now beginning to be available. The most widely used agents involve DTPA, glucoheptonate (see Figure 5) and DMSA [8].

In the blood, the penicillamine complex is largely protein bound and is consequently taken into the renal cortex and excreted only very slowly in the urine. It yields high kidney-to-background images and its accumulation in the kidneys correlates well with differential inulin clearance and with the ERPF. The complex can exist in two diastereomeric forms, when prepared from $[OCl_4Tc^{V}]^-$ and racemic penicillamine in concentrated HCl [100]. A crystal structure of the form prepared with D-penicillamine alone reveals an octahedral complex containing the $[Tc{=}O]^{3+}$ core with two penicillamine ligands (see Figure 6). One is bidentate with sulfur and nitrogen coordination *cis* to the oxo, while the other is tridentate with *cis* coordination of the thiolate and amine and the

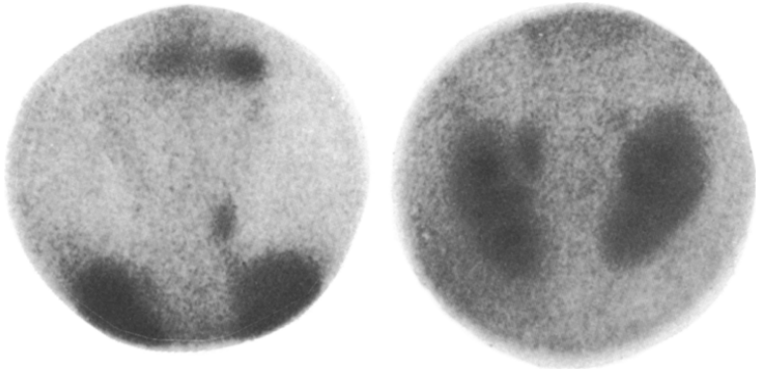

Fig. 5 Renal image revealing kidney masses taken 10 min. after injection with ^{99m}Tc-glucoheptonate complex. (*Courtesy, DuPont, NEN Products*).

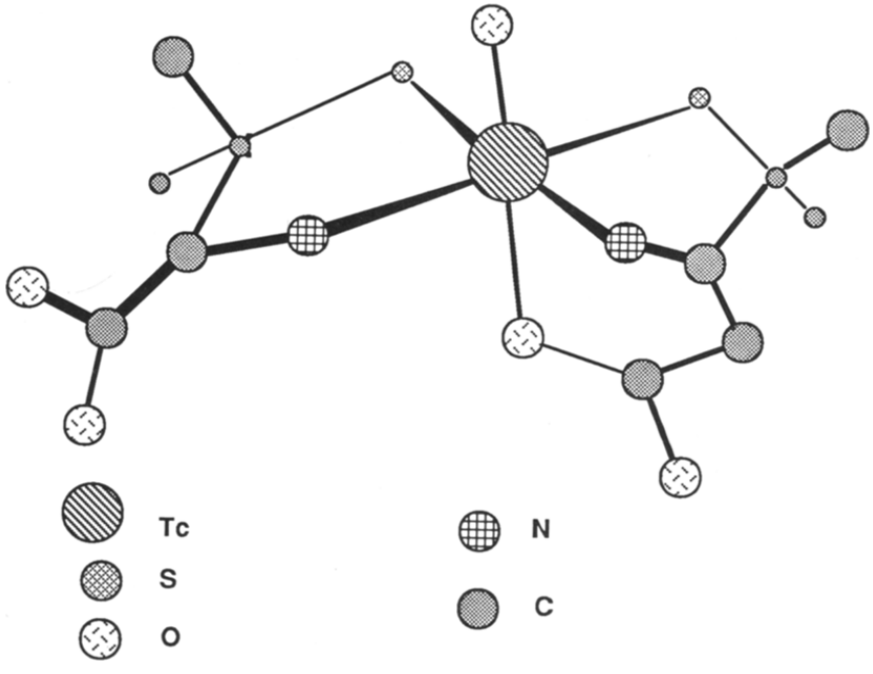

Fig. 6 Structure of 1-oxo-2,3,6-(D-penicillaminato-N,S,O)-4,5-(D-penicillaminato-N,S)technetium(V) [101].

carboxylate binding *trans* to the oxo. Owing to the method of preparation, the molecule is neutral with the free carboxyl group protonated. However, deprotonation of this site above pH 3.0 undoubtedly contributes to its water solubility. Its diastereomer occurs when both a D- and L-penicillamine are coordinated. Since the carboxylate on either enantiomer can be coordinated, two complexes are possible [101]. While this generates an enantiomeric pair, carboxylate exchange is facilitated by the *trans* effect of the oxo ligand. Consequently, enantiomeric interconversion is sufficiently rapid that an effective plane of symmetry results yielding a fluxional molecule on the NMR time scale at room temperature. It is possible that this rapidly exchanging site provides the initial coordinating position for the complex to become protein bound and so may be partly responsible for its mode of renal clearance. A complex made with penicillamine ethyl ester was shown to be lipophilic with hepatobiliary uptake and able to enter red blood cells and bind internally [102].

The ^{99m}Tc-DTPA imaging agent is nearly quantitatively handled by the kidneys. It is filtered at the glomerulus almost exclusively with a single-pass efficiency of 20%. This feature has made it popular not only for routine renal scanning, but also for quantitative measurements of renal function, especially determination of the GFR. Since it can be administered in large quantities, it has further been used for the semiquantitative analysis of ureter drainage. While no definitive structural studies on the DTPA complex have been made, structures are available on presumably closely related EDTA species.

Slow bisulfite reduction of a warm solution $HTcO_4$ in the presence of EDTA results in crystals formulated as $[(H_2EDTA)Tc(\mu\text{-}O)_2Tc(H_2EDTA)]\cdot 5H_2O$ on cooling [103]. Sites opposite the bridging oxo ligands are occupied by amine nitrogens, while the two remaining positions are coordinated by carboxylates (see Figure 7). Two acetate fragments of each EDTA are not involved in ligation and hydrogen bond with waters of hydration. Given that the Tc-O-Tc bond angles are 75°, it is possible that the bridges are actually hydroxyls, rather than oxo ligands. If this is the case, then the technetiums would be assigned as Tc(III) instead of Tc(IV). Unfortunately, there is no clear spectroscopic difference between

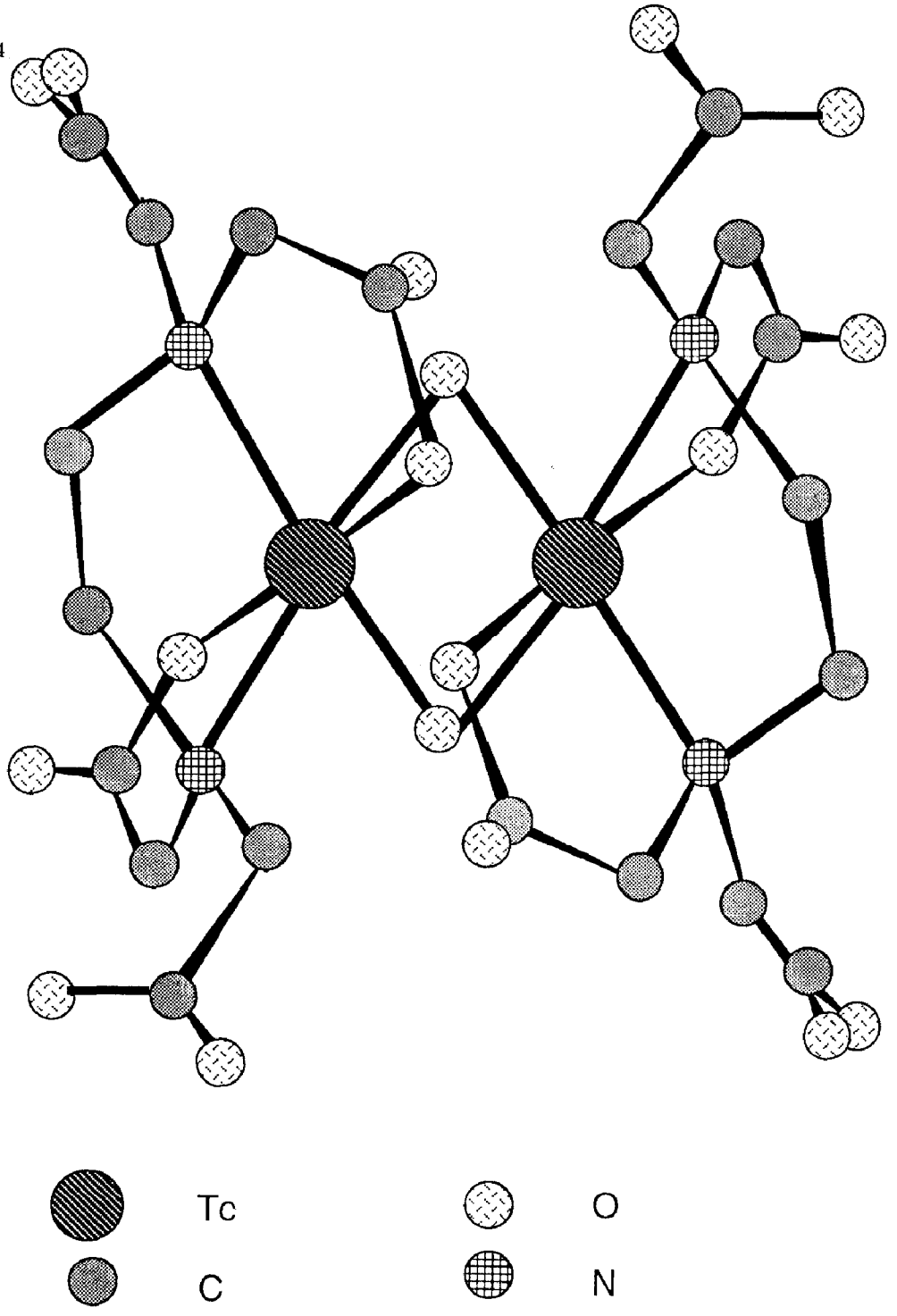

Fig. 7 Structure of $[(H_2EDTA)Tc(IV)(\mu\text{-}O)_2Tc(IV)(H_2EDTA)].5H_2O$[103]

these two structures. The short Tc-Tc distance of 2.33 A suggests a bimetallic multiple bond. Determination of this as a double or triple bond depends on the correct assignment of the Tc oxidation states. An alternate synthesis involves the reduction of $[TcO_4]^-$ with $NaHSO_3$ in the presence of EDTA to yield a gold complex, presumed to be a Tc(III) intermediate. Slow oxidation of the gold species with H_2O_2 followed by addition of $HClO_4$ yields an analytically pure product in 84% yield, while rapid oxidation produces a second, possibly mono-oxo bridged species, that slowly converts to the bis μ-oxo complex [104].

A similar binuclear species with nitriloacetic acid (NTA) results from sulfur dioxide reduction of $HTcO_4$ at pH 2 and has been formulated as $Na_2[(NTA)Tc(\mu\text{-}O)_2Tc(NTA)]\cdot 6H_2O$. Each NTA is tetradentate on separate technetiums. The molecule has an inversion center with approximate C_{2h} symmetry and a Tc-Tc separation of 2.363 A (see Figure 8) [105]. The reaction of $K_2[TcBr_6]$ with NTA in 1 M HBr or the reduction of $[TcO_4]^-$ with Sn(II) in the presence of NTA yielded two apparently oligomeric products: a red species, which analyzed as $K_2[O(NTA)Tc]_2\cdot 2H_2O$ and a brown compound consistent with $[K_3H_2[Tc_3O_2(OH)_4(NTA)_3]\cdot 6H_2O]$ [106].

Monomeric Tc(V)-EDTA complexes are also possible. The reaction of $(n\text{-}Bu_4N)[OCl_4Tc]$ with H_4EDTA in anhydrous DMSO produces $[O(EDTA)Tc]^-$ in nearly quantitative yield [9,10,107]. The barium salt has been crystallized and studied by x-ray crystallography (see Figure 9). In this compound each technetium atom is seven coordinate in a distorted pentagonal bipyramidal structure with two EDTA carboxylates occupying the axial sites and the other two carboxylates, the two amines and the oxo bound equatorially. Since the two amine nitrogens are approximately opposite the oxo ligand, their bond distances to the Tc are somewhat lengthened (2.35 A) by the trans influence exerted by the oxygen [10]. Reaction of $K_2[TcBr_6]$ in 0.1 M HBr yielded a product also suggested to contain the $[Tc{=}O]^{3+}$ core, but with two pendant carboyxlates (μ_{eff} = 1.53 β, θ = -54 K, $\upsilon_{Tc=O}$ = 925 cm^{-1}) [108].

It has been suggested that DTPA forms both mono- and binuclear complexes upon reacting with $[TcBr_6]^{2-}$. The mononuclear species was formulated as $H_3[O(DTPA)Tc]\cdot 2H_2O$ (μ_{eff} = 2.4 β, θ = -32 K,

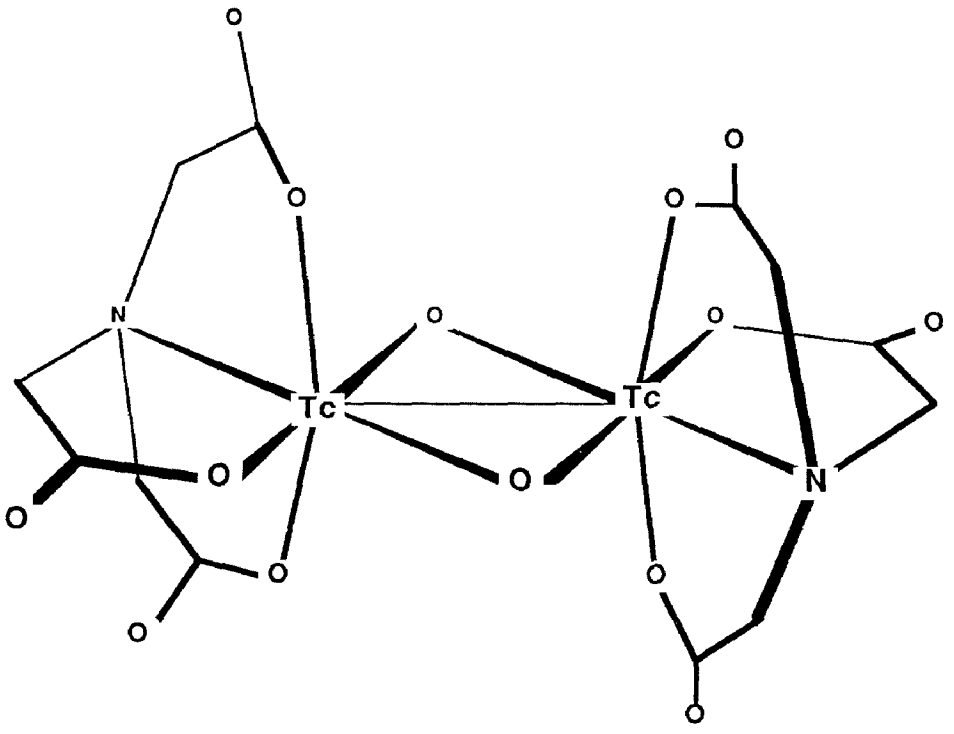

Fig. 8 Structure of $Na_2[N(CH_2COO)_3Tc(\mu\text{-}O)_2TcN(CH_2COO)_3].6H_2O$ [105].

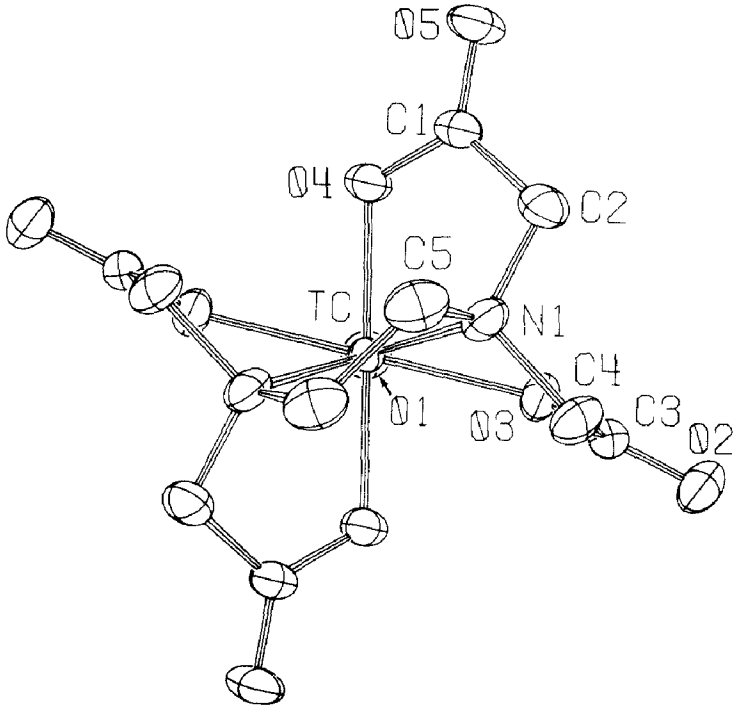

Fig. 9 Diagramatic structure of $[O(EDTA)Tc]^-$ showing essential features of coordination [see references 9,10 and 107].

$\nu_{Tc=O}$ = 920 cm^{-1}). Titration indicated three uncoordinated carboxylates on the complex [107]. Heating micromolar solutions of this at neutral pH resulted in a brown product suggested to be $[(DTPA)Tc\text{-}O\text{-}Tc(DTPA)]^{6-}$ (μ_{eff} = 1.47 β, θ = 0 K.) The exclusive glomerular filtration of the DTPA agent and its avoidance of tubular or protein binding is probably due to the chelating ligand's covering all possible coordination sites. In this respect it significantly differs from the penicillamine, DMSA and glucoheptonate species, while retaining the $[Tc=O]^{3+}$ core. The pK_{assoc} for the presumably monomeric complex has been reported as 26.3 [109]. Unlike the ema complex (see below), the presence of the pendant carboxylates probably enhances its hydrophilicity and so minimizes its uptake by the bile.

The complex $[O(ema)Tc]^-$ (ema = N,N'-ethylenebis(2-mercaptoacetimide) is formed virtually quantitatively from $[TcO_4]^-$ at both carrier (10^{-5} M) and no carrier added (10^{-8} M) levels. This and similar N_2S_2 chelates are extremely effective in sesquestering technetium and their *in vivo* stability makes them promising as renal imaging agents. Animal studies show the complex is rapidly cleared into the urine [96]. Significant excretion into the bile and feces also occurs without localization or reabsorption of the radioactivity. HPLC and mass spectrometry of the activity excreted into the urine reveals that the complex is eliminated intact and is not degraded to pertechnetate. Biodistribution is essentially the same at both the carrier-added and no-carrier added levels.

Synthesis of the ema complex involves using the benzoyl derivative to protect the thiols, which is placed in 1 M NaOH to effect dissolution. Pertechnetate is then added with sodium dithionite as the reductant and the mixture heated to boiling. Reverse phase HPLC (on a C_{18} column eluted with a water/methanol gradient containing 5 mM tetra-n-butylammonium phosphate) and spectroscopic analysis showed no evidence of TcO_2 formation and only a small amount of unreacted $[TcO_4]^-$. Field-desorption mass spectrscopy (FDMS) revealed two peaks corresponding to an intact ion cationized by the addition of two protons (m/z = 321) and a weaker molecular cation peak (m/z =561), with the technetium ion's weight being determined at 319 [98].

An x-ray determination of the structure of the ion (see Figure 10) shows it to be square pyramidal with equatorial coordination to the two sulfur and two nitrogen atoms of the ema. The Tc≡O bond length is 1.672 A, with the Tc atom being 0.771 A above the plane of the ema ligand atoms. The ema moiety also exhibits some ruffling to accommodate the Tc. Since the prototype complex is also excreted by the bile and its urinary clearance is markedly affected by a depression of renal function, derivatives are now being developed and tested [97]. Several isomers with respect to the location of the amide function have been prepared and are all quite stable in aqueous solution. The presence of the apical oxygen makes the methylene protons diastereotopic. When the methylene groups are adjacent to a carbonyl in a five-membered ring, they rapidly undergo highly stereospecific deuterium exchange in basic D_2O [110]. Carboxylate substitution on the ligand also results in epimers, one of which appears to have superior characteristics for renal imaging. The problem of stereoisomers has been obviated by replacing one sulfur with an effectively planar amido nitrogen. These triamide mercaptide complexes (N_3S) such as $[O(MAG_3Tc]^{2-}$ (MAG_3 = mercaptoacetylglycylglycylglycine) are rapidly excreted in the urine and are likely to be employed clinically [111].

The DMSA complex also probably posseses the basic square-pyramidal geometry with an apical oxygen and sulfurs in the basal plane. It is well suited for renal scanning and is also used to assess renal function. In the blood, the complex is substantially protein bound and so is not filtered by the glomerulus. Instead it is transferred from the efferent arteriole to the peritubular capillary. From the blood capillary it enters the tubule and becomes fixed, presumably to sulfide and sulfhydryl sites on the tubular wall. Its maximum renal concentration, which is about half of the administered dose, is reached in 2-4 hrs. and almost all of this (96%) is localized in the renal cortex. Owing to this high degree of retention, it is optimal for imaging the morphology of the cortex. Renal scanning with ^{99m}Tc-DMSA provides a sensitive early indication of parenchymal scarring in children with pyelonephritic changes [112]. Since its accumulation by the kidneys is proportional to the ERPF, it has also been used for renal functional evaluations.

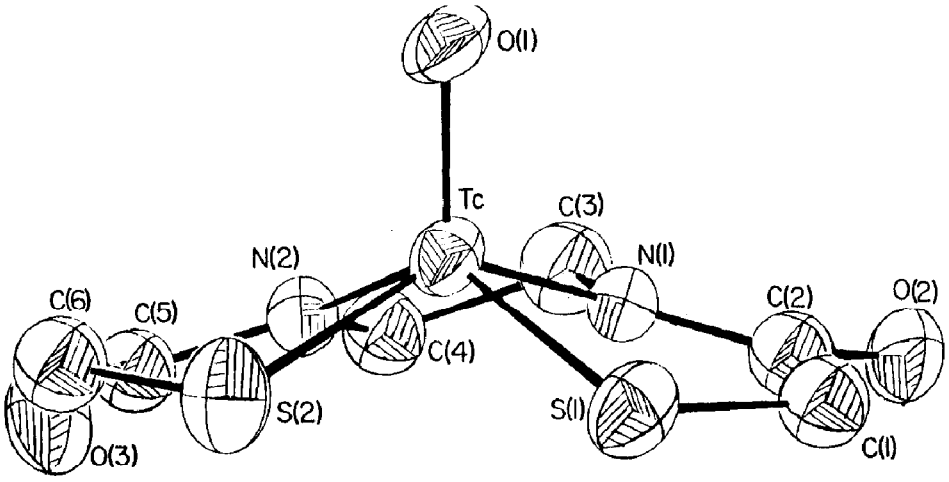

Fig. 10 Structure of oxo[N,N′-ethylenebis(2-mercaptoacetimido)]Tc(V) [97].

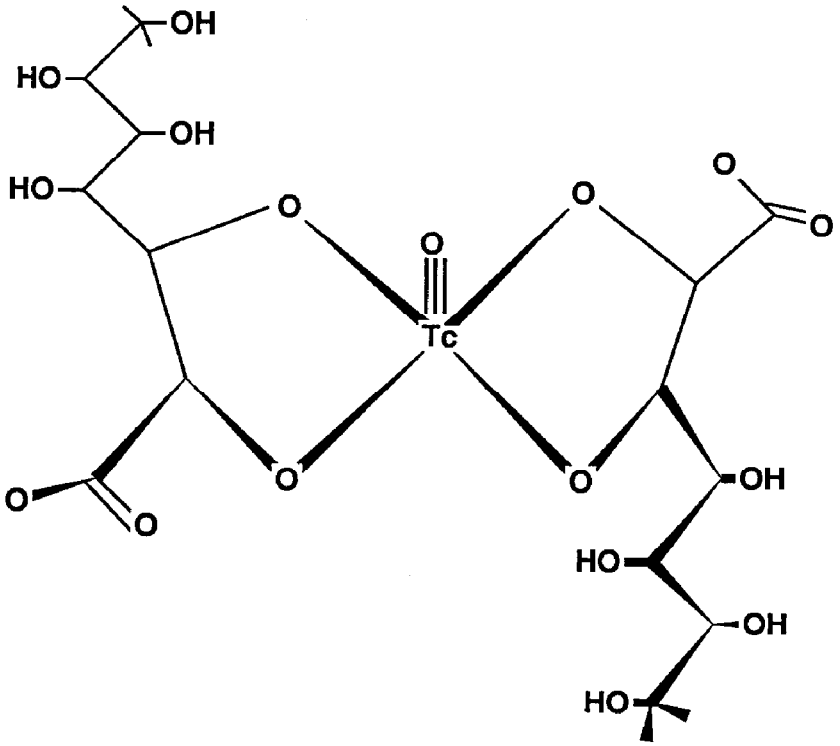

Fig. 11 Proposed structure of [O(glucoheptonate)$_2$Tc]- [113, 263].

The glucoheptonate complex enters the renal tubule by both filtration and secretion and exhibits about 25% binding to the tubule, with the remainder being excreted in the urine. Because of this distribution in its renal handling, it has not been useful for quantitative evaluations and has been restricted to morphological studies and the qualitative assessment of renal blood flow [85]. The compound is prepared by Sn(II) reduction of $[TcO_4]^-$ in the presence of a 25-molar excess of the ligand. It is quite stable at neutral pH, exhibits a weak visible absorbance at 502 nm (ϵ= 65 M^{-1} cm^{-1}), and has a charge of -1. Job's plots have indicated two ligand molecules per Tc; however, more recent work suggests a 1:1 ratio [263]. The infrared spectrum exhibits Tc≡O stretches at 930 and 970 cm^{-1}. The similarity of the electronic spectra to that of the ethyleneglycol complex suggests suggest hydroxyl binding [63, 263] and evidence for this is also present in NMR [113]. Presently, it is not clear whether the best formulation for the glucoheptonate complex at neutral pH is $[O(gluco)_2Tc]^-$, which is most likely square pyramidal involving diolato (see Figure 11) or olato and carboxylato coordination, or if a μ-oxo dinuclear species occurs with one glucoheptonate for each Tc. Coordination of water, hydroxyl or even a carboxylate group opposite the oxo is also possible and would provide additional stabilization. A pertinent diolato comparison structure is that of the catecholato complex, which shows the Tc to be coordinated in a square pyramidal geometry with an average Tc-O(catecholato) distance of 1.954 A [63].

Several studies have shown that bisthiolato complexes are easily prepared by ligand exchange from the Tc(V)-gluconate complex in alcohol or water/alcohol mixtures [114 ,115 ,116]. Preparation of the 2,3-dimercaptopropanesulfonate complex in this manner [62] yielded a spectrum identical to that of $[O(SCH_2CH_2S)_2Tc]^-$, whose structure is of the typical square-pyramidal variety [117]. Such reactions are certainly pH-dependent, since proton addition catalyzes the loss of alcoholate ligands. Similar substitutions involving protein thiolate groups may account for the partial binding of the glucoheptonate complex to renal tubules. Electrophoresis of the products formed between $[^{99m}TcO_4]^-$ and several 1,3-dimercapto ligands verifies the 1:2 stoichiometry, since reactions with two ligands present revealed a product distribution of 1:2:1, with the new compound formed being twice as abundant as those formed in the presence of either ligand alone [118].

Bone Imaging Agents. The introduction in 1971 of ^{99m}Tc complexes of linear polyphosphates ushered in a new era for scintigraphic techniques in nuclear medicine [119]. Since only ^{18}F, ^{85}Sr and ^{87m}Sr had been available for bone imaging, this event greatly improved the quality of skeletal images. The early agents were expensive, with ^{18}F requiring a nearby cyclotron for synthesis and the strontium complexes giving a very high background. Drawbacks of the initial tripolyphosphate and polyphosphate agents derived from variations in chain lengths of the polyphosphate compounds and slow blood clearances [120 ,121 ,122]. Complexes with pyrophosphate, which appeared to be the functional agent in the polyphosphate preparations,[123] and ethane-1-hydroxy-1,1-diphosphonate (HEDP) [124] were introduced shortly thereafter and exhibited superior imaging characteristics. Newer agents involving imidodiphosphate [125], methylene diphosphonate (MDP),[126], and hydroxymethylene diphosphonate (HMDP) [127] were more stable and so exhibited a more specific and reproducible biodistribution together with a more rapid blood clearance. These features provided a higher bone to background ratio and so improved image quality. Clinically used kits contain a mixture of $SnCl_2$, an antioxidant, such as sodium ascorbate, and the diphosphonate ligand. The efficacy of bone agents is profoundly sensitive to their conditions of preparation. Important factors are the technetium concentration, pH, concentration of the ligand, the ratio of ligand to tin and the amount of tin used [128]. A range of products is often produced with most being oligomeric or polymeric.

Phosphonate Ligands

$[O_3P-O-PO_3]^{4-}$	$[O_3P-CH_2-PO_3]^{4-}$	$[O_3P-\underset{\displaystyle OH}{\underset{\vert}{CH}}-PO_3]^{4-}$	$[O_3P-\underset{\displaystyle CH_3}{\underset{\vert}{\overset{\displaystyle OH}{\overset{\vert}{C}}}}-PO_3]^{4-}$
Pyrophosphate	**MDP**	**HMDP**	**HEDP**

Radioscintigraphic bone imaging is extremely sensitive to localized abnormalities in the skeleton; however, since uptake of the agent usually depends on increased metabolic activity, it is fairly nonspecific as to the cause of the uptake. For example, it is almost impossible to tell from a bone scan alone whether a

visible "hot spot" is due to an inflammatory infection, a microfracture, a primary bone cancer or a metastasized cancer [129]. Pediatric patients, with rapidly growing bones and skulls, show increased uptake in the cranial sutures and intense accumulation in the epiphyses of the bones, which can obscure sites of infection or fracture. Because of these considerations, diagnostic accuracy is often improved by correlating the scintigraphic results with radiographic (x-ray) studies of the same area. This is particularly true in scans in the area of the pelvis because isotope accumulation in the bladder following renal excretion tends to obsure portions of this region [130].

^{99m}Tc-labeled sulfur colloid (see below) is a specific scanning agent for the early diagnosis of osteonecrosis. Since this agent is taken up by viable bone marrow, a unilateral deficiency of activity is indicative of decreased blood supply and implies the presence of osteonecrosis [130]. In its early stages this disease may also be indicated by a "cold" or photon-deficient area on a ^{99m}Tc-phoshponate bone scan. However, at a later stage, after revascularization and bone repair have started, the scan may show increased activity in the same area [131].

Similar changes in bone scans may be evident in osteomyelitis, an infection of the soft, inner portion of the bone. Since incorporation of ^{99m}Tc depends on blood flow to the affected area, accumulation will not occur at localized sites of osteomyelitis around which thromboses have occured to block local capillaries and arteries. Conversely, the scan may show abnormal activity after the infection has subsided and bone repair is progressing [132]. Bone scans are very effective in localizing occult osteomyelitis, which may be the source of fever of unknown origin in infants, or detecting this disease in drug abusers, who frequently have unusual sites of skeletal infections [130].

Radioscintigraphs are often performed when radiographs are negative, but it is clinically suspected that a fracture is present. The uptake of ^{99m}Tc-bone agents increases with time in recent fractures and then slowly decreases as healing subsides. Bone scans are positive as soon as 7 hr after fracture and reveal 60% of suspected stress fractures before radiographic signs are

present. Successive negative scans essentially preclude fracture as a diagnosis. Bone scanning is also useful in detecting mechanical loosening or infection after a total hip replacement, in the diagnosis of Paget's osteogenic sarcoma, and in evaluating the response of this disease to treatment [130]. Since bone agents are usually rapidly excreted, the kidneys and bladder are routinely visualized and abornormalities of these organs are often serendipitously discovered. Soft tissues may also show activity in areas where calcification is taking place [133].

In substituting an aliphatic carbon for the oxygen bridge in pyrophosphate, the *in vivo* stability of the molecule is enhanced, since the array of body enzymes that rapidly hydrolyze the P-O-P backbone do not attack phosphonates. The phosphonate ligands retain a high affinity for calcium, even though they are already coordinated to technetium. The pyrophosphate and diphosphonate complexes are not specific for bone, but accumulate wherever there is deposition of calcium phosphate. It has been suggested that diphosphonates in general, but especially HMDP and HEDP add to the rapidly growing faces of nascent hydroxyapatite crystals in bone [134]. Since hydroxyapatite crystals grow rapidly along the **c**-axis, addition occurs most readily at the 001 faces. As a result of rapid growth along the **c**-axis, the 001 faces gradually contribute less to the exposed surface of the crystal. Owing to their tridentate structure deriving from the two phosphates and the central hydroxyl, HMDP and HEDP are well suited to bind preferentially to the 001 faces, and so may be fairly specific for new bone relative to older bone whose 001 crystalline faces have been diminished (see Figure 12).

The affinity of *coordinated* diphosphonate ligands for Ca^{2+} has been measured using a series of complexes, $[(en)_2(DP)Co]^-$ (where DP = $[O_3P\text{-}CRR'\text{-}PO_3]^{4-}$) at pH 10. Association constants for the ligands with R/R′ combinations of H/H and H/OH were 1.8 x 10^4 and 2.4 x 10^6, respectively [135]. These values indicate that coordinated diphosphonate ligands exhibit considerable affinity for Ca^{2+} and that this is substantially enhanced by the presence of the hydroxyl. Moreover, the ordering of affinities exactly parallels the ordering of skeletal uptake of the ^{99m}Tc MDP, HMDT and HEDP complexes. These results strengthen the supposition that these

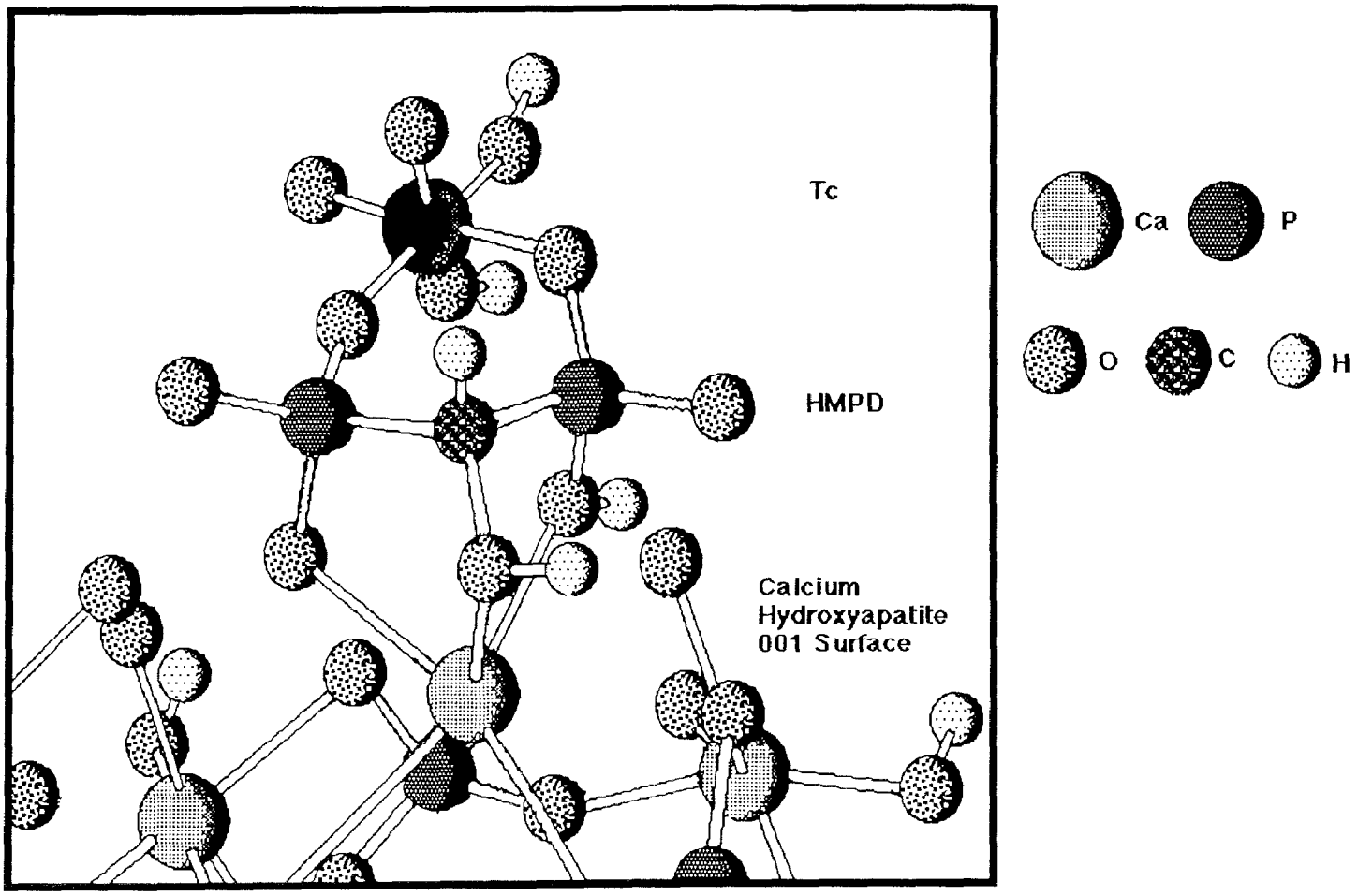

Fig. 12 Proposed structure of Tc-HMDP complex adding to the 001 face of calcium hydroxyapatite.

ligands form a bridge between the Tc and Ca ions on the surface of hydroxyapatite.

Diphosphonate ligands tend to form polymeric metal complexes and the ability of MDP to function as a doubly bidentate bridge is illustrated by the structure of a polymeric Tc-MDP complex in which the MDP bridges two Tc centers [136]. When the diphosphonate has a central hydroxyl, it can also function as a bidentate-tridentate bridge between two metal ions. In the case of the bone-imaging agents, the Tc is probably bound to the terminal phosphates in a bidentate fashion, while the Ca^{2+} on the crystal surface is bridged to the Tc in a tridentate manner by both the phosphates and the hydroxyl (see Figure 12) [137]. In the single crystal structure of the Tc-diphosphonate complex, it is not clear if the metal exists as Tc(IV) or Tc(V); however, it is generally thought that Tc(IV) predominates in most agents. The compound has the empirical formula $Li(H_2O)_3[Tc(OH)(MDP)]\cdot 1/3H_2O$ and consists of infinite polymeric chains containing two symmetry related, six-coordinate Tc ions bridged by a hydroxyl and each coordinated by two symmetry related MDP ligands. The Tc-O distances are all in the range expected for single bonds with the Tc-O(phosphate) bond lengths being between 1.96 Å and 2.03 Å and the Tc-O(hydroxyl) bond being 1.912 Å.

HPLC analysis of the products of clinically used "kits", have shown them to be mixtures of several components [138]. Reduction of 3 mM $[TcO_4]^-$ by sodium borohydride (rather than Sn^{2+}) in the presence of HEDP resulted in a mixture of at least seven different ^{99m}Tc-HEDP complexes. However, when the reaction was run with no carrier added $[^{99m}TcO_4]^-$, essentially only one complex was evident [139]. This suggests that oligomeric and polymeric species are being formed at the higher concentrations. Since polymer formation generally proceeds by higher-order kinetics, these reactions are slow at the lower (no carrier added) concentrations, where monomer formation is favored. Owing to the similar size of Tc(IV) and Sn(IV) (0.65 Å and 0.69 Å, respectively)[4], these two ions often form structurally similar complexes and it is likely that the polymers formed contain both tin and technetium [140].

The various species separated by HPLC exhibited differing levels of bone and soft tissue uptake. The first component eluted in this chromatographic system showed the highest bone and lowest soft tissue uptake, while the last species eluted showed the lowest bone and highest soft tissue uptake. In general, a negative correlation exists between the "charge density" of the radiopharmaceutical as measured by the logarithm of its chromatographic retention time and its bone uptake. It may be that the negative charge on the complex (i.e. its polarity), determines both the strength of its ion-pairing with reverse-phase materials and its affinity for polar sites on the faces of hydroxyapatite crystals [141].

Hepatobiliary Agents. The liver is the largest organ in the body and receives about 20% of the resting cardiac output. It provides a variety of metabolic functions including the removal of foreign bodies from the blood through phagocytic cells (Kupffer cells) situated along the lining of the hepatic sinusoids. The metabolic function occurs primarily in the parenchymal cells (hepatocytes), which comprise 60% of the liver cells and about 90% of the liver mass. Excretion into the bile is the most important elimination pathway and plays a major role in the removal of both ionic and neutral molecules over 300-500 but under about 5000 in molecular weight. Molecules comprised of a nonpolar moiety coupled to a highly polar side chain may resemble the bile salts, which are steroids linked to polar glycine or taurine residues. Some molecules are oxidized by the liver and/or conjugated to polar groups such as glucuronic acid, which provides a soluble species that can be excreted by the kidneys. Separate membrane-bound active-transport carriers exist in the hepatocytes for the intake of anions, cations, neutral molecules and bile salts. Bile may directly enter the duodenum or it may flow into the gallbladder, where it is concentrated, stored and subsequently passed into the intestines by gall bladder contraction [142]. The clinical utility of hepatobiliary imaging agents is based on their ability to produce liver images which: a) reflect the distribution of functional hepatocytes, b) outline the biliary tract, and c) trace the pathway of bile flow or leakage. Imaging techniques now insure that very few patients will be subjected to unnecessary exploratory abdominal surgery (laparotomy) in order to diagnose an hepatic disorder.

^{99m}Tc-labeled sulfur colloids (discussed below) with sizes between 0.3-1.0 μm are rapidly taken in by the Kupffer cells. Imaging with these particulates is useful in delineating the morphology of the liver and may define varying degrees of liver injury following wounds to the abdomen [143]. Hepatic imaging with radiocolloids is easily performed, exhibits a high sensitivity for the detection of liver disease, and is extremely effective in distinguishing between cirrhosis and metastases [144 ,145]. An inhibited hepatic reticuloendothelial system will result in a poorly imaged liver and may be evident in a variety of illnesses in which blood flow to the hepatic sinusoids, where the most efficient trapping of particles occurs, is disturbed. It has also recently been used to predict the response of hepatic cancer patients to chemotherapy injected directly into the hepatic artery. Since this chemotherapeutic technique is effective only if the drug is efficiently extracted on its first pass through the liver, an imaging technique which accurately reflects blood perfusion patterns through the liver provides a good indication of drug distribution and, hence, probable drug response [146].

Hepatobiliary imaging agents should exhibit a high initial intake by the liver and rapid excretion into the bile. Since these agents are taken up by the liver via active transport into the hepatocytes, their uptake exhibits non-linear Michaelis-Menten profiles and may reach a saturation limit. The presence of other materials, such as bilirubin, which are transported by the same anion transport sites, can also inhibit the uptake of a given radiotracer. Quantitation of hepatocyte function is optimal in an agent whose uptake is independent of competing levels of blood bilirubin, which are often high in liver dysfunction [142,143].

In general, hepatobiliary imaging agents are lipophilic compounds with sufficient polarity to be water soluble. In the mid 1950's ^{131}I-rose bengal was developed as the first imaging agent for hepatic function and proved to be especially useful in differentiating between hepatocellular disease and bile duct obstruction. However, since only relatively small doses could be employed, it was less than optimal for detecting biliary leakage [147]. Replacements were sought which would provide for higher photon counts and more efficient clearance from the blood. While a

Normal Hepatobiliary Imaging Anatomy

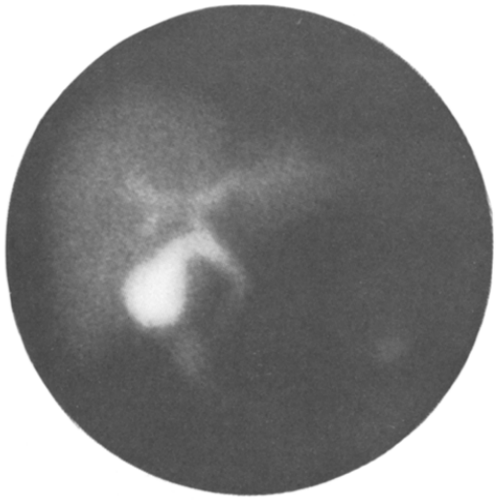

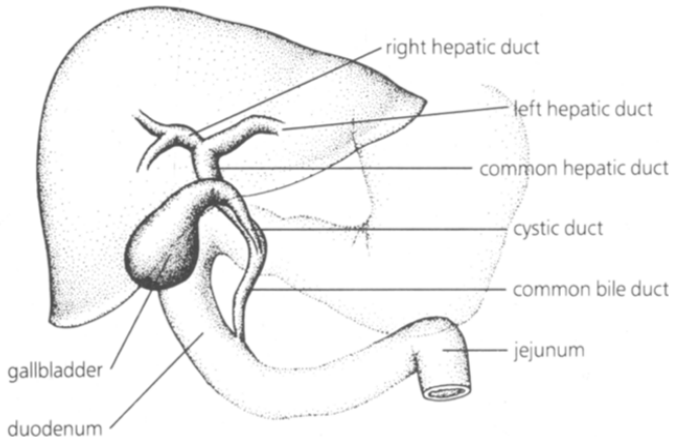

Fig. 13a Image of a normal liver and gall bladder 20-25 min after injection with ^{99m}Tc complex of N-(2,6-dimethylphenylcarbamoylmethyl)iminodiacetic acid. Diagram indicates positions of the various structures visualized.

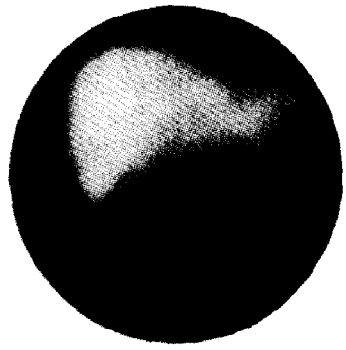

10 min

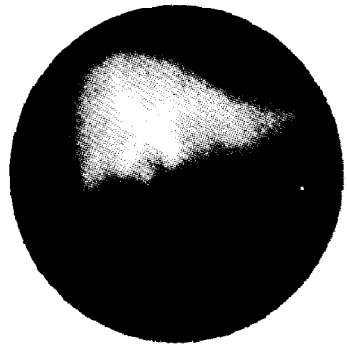

30 min

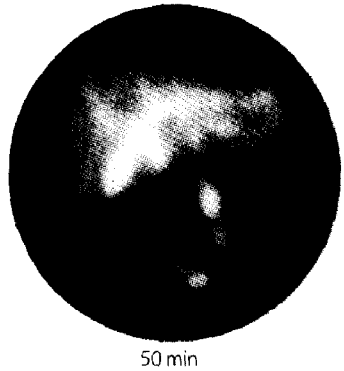

50 min

Fig. 13b Hepatobiliary images at varying lengths of time after injection revealing a partial common duct obstruction. (*Courtesy, DuPont, NEN Products*).

variety of ^{99m}Tc-complexes were tried, this goal was serendipitously attained by Loberg and coworkers (see Figure 13) who were seeking a heart-imaging agent by developing analogs of the antiarhythmic drug, lidocaine, which was known to accumulate in the heart [148 ,149]. Some success was also met with complexes of pyridoxylidene glutamate and similar Schiff base ligands made with other amino acids [150].

The original preparation of the Schiff base complexes involved heating the amino acid, pyridoxal and $[^{99m}TcO_4]^-$ at pH 8. It has been suggested that the pyridoxal aldehyde group reduces the $[TcO_4]^-$ to Tc(IV) before Schiff base coordination occurs. The ligand presumably involves an imine link formed between the pyridoxal carbonyl and the amino group of the amino acid. Running the reaction in this manner produces several side products, including colloids [151]. These materials have not been structurally characterized and some are excreted by the kidneys. An improved preparative method used Sn(II) in the presence of ascorbate as the reductant and produced a single radiochemical product [152]. TLC, ion exchange and electrophoretic analysis analysis of the products formed using mixtures of pyridoxylideneisoleucine (PI) and pyridoxylideneglutamate (PG) in varying ratios are consistent with the formation of $[(PI)_2Tc]$, $[(PI)(PG)Tc]^-$, and $[(PG)_2Tc]^{2-}$ (see Figure 14) [153].

Structural studies have recently been performed on other Schiff base complexes synthesized by the additon of the ligand to $[n\text{-}Bu_4N][OCl_4Tc]$. In the complex $[O(H_2O)(acac_2en)Tc]^+$ (where $acac_2en$ = N,N'-ethylenebis(acetylacetone imine)) the Schiff base occupies the equatorial positions with an apical oxo *trans* to the water. The molecule *trans*-$[OCl(sal_2en)Tc]$ is similar, but with a chloride occupying the position opposite the oxo [45]. The Tc-O bond distances are around 1.648 A and 1.626 A, in the two complexes, respectively, indicating partial triple bonding. The spectra of these complexes are solvent dependent, which probably reflects the presence of different solvent ligands occupying the site *trans* to the oxo. In the structure of $[OCl(Phsal)_2Tc]$ (where Ph-sal = N-phenylsalicylideneimine), which was made by refluxing $[AsPh_4][OCl_4Tc]$ and the ligand in ethanol, the oxo and chloride are *cis* to one another. The Schiff base ligands are orthogonal to each other with a phenolic oxygen *trans* to the oxo ligand [154].

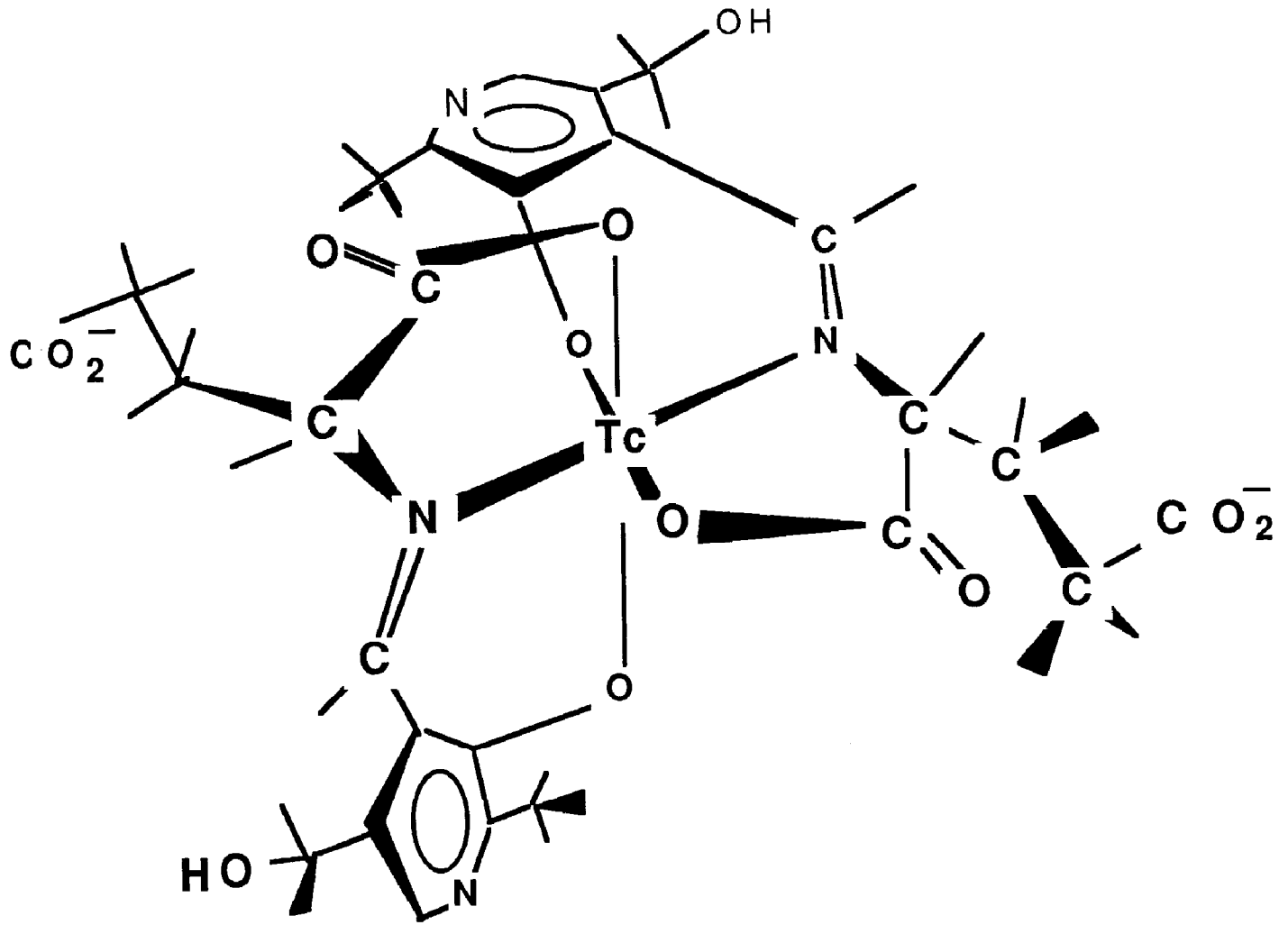

Fig. 14 Diagramatic structure of the liver-imaging agent $[(PG)_2Tc]^{2-}$ showing essential features.

Necessary structural features of the pyridoxylidene liver imaging agents, which are not reflected in the above structures, are: a) a phenolic oxygen at the 3-position of the pyridoxal, b) an electron withdrawing group in the pyridoxal capable of extended conjugation, and c) an amino acid. The facile synthesis and the general stability of the Schiff-base complexes suggest that hepatobiliary uptake might be improved by increasing the lipophilicity of the ligand as measured by the n-octanol/water partition coefficient of the complex [155]; however, it is not clear that this would offer any significant advantage over the widely used iminodiacetate complexes.

Iminodiacetates (IDA's) are excellent sequestering agents and can be likened to "half an EDTA" in their chelating ability. The first complex involved the stannous reduction of $[^{99m}TcO_4]^-$ in the presence of dimethyl-HIDA (HIDA = 2,6-dimethylphenylcarbamoylmethyl iminodiacetic acid), which is structurally similar to lidocaine [156]. The rate of complexation increases with increasing acidity and ligand concentration, but is independent of the Sn(II) concentration. The free ligand is subject to rapid renal excretion, while the ^{99m}Tc-complex is concentrated by the liver and is then excreted throught the hepatobiliary system [157].

Clinically used IDA complexes are quite stable and are excreted unmetabolized. A variety of IDA derivatives and analogs have now been evaluated for clinical use. In addition to having a size, polarity and molecular weight suitable for hepatobiliary uptake, essential features of ^{99m}Tc-IDA complexes are:

a) An amine-diacetate function (with an amine pK_a around 6) for metal complexation.
b) An electron withdrawing subsitutent on the β-carbon from the amine to modulate the basicity of the amine.
c) A lipophilic group tethered at a substantial distance from the amine-diacetate.

In the case of tethered phenyl groups (see Figure 15), *ortho* substitutents appear to affect hepatic uptake, while *para* groups seem to modulate binding to blood proteins. Increasing the bulk of the *ortho* substituents causes variations in the labeling rate, stability and the number of products formed [148]. These may be due to the formation of an intermediate complex, which is more

slowly converted to the final product as the steric bulk of the ligand increases. Complexation kinetics are biphasic with a rapid ligand concentration-dependent initial phase being followed by a slower concentration-independent reaction. Decreasing the basicity of the amine nitrogen by substitution of electron withdrawing groups such as the benzoyl moiety, results in unstable complexes [158].

Hepatocyte uptake of ^{99m}Tc-IDA complexes is inhibited by bromosulphthalein, bilirubin and taurocholate, which also inhibit uptake of ^{131}I-rose bengal; but cationic compounds show no inhibition. This suggests that the anionic compounds are all subject to the same active transport mechanism. The dimethyl-HIDA derivative has the least hepatobiliary specificity, which improves on going to the diethyl derivative. The diisopropyl-HIDA complex has uptake kinetics similar to the diethyl derivative, but is more resistant to high serum bilirubin levels. The fraction of material excreted into the bile has been shown to be linearly related to its charge density, defined as the log of the molecular weight of a complex divided by the charge [159]. The *para*-butyl derivative is cleared more rapidly from the blood, but is excreted only slowly by the liver into the bile. A clinical study may involve an initial dynamic study, with routine images being taken at one and five minutes, sequentially followed by images at 5 min intervals up to an hour and then for each hour for three additional hours [145, 160].

Unfortunately, there is no clear picture as to the structure of the ^{99m}Tc-IDA agents. Early HPLC studies led to the conclusion that the HIDA complex was formed almost quantitatively and electrophoretic experiments indicated a monoanionic complex with a stoichiometry of two HIDA ligands for each Tc. The oxidation state was determined by the titration of excess stannous ion in the reaction mixture with iodine [149]. On this basis, the formulation was suggested to be $[(HIDA)_2Tc(III)]^-$ in a presumably octahedral complex (see Figure 15) [161]. While confirmation of this structure has been provided by fast atom bombardment mass spectrometry [99], IDA ligands are not expected to delocalize sufficient electron density away from the Tc to stabilize the Tc(III) oxidation state. An alternative suggestion is that the

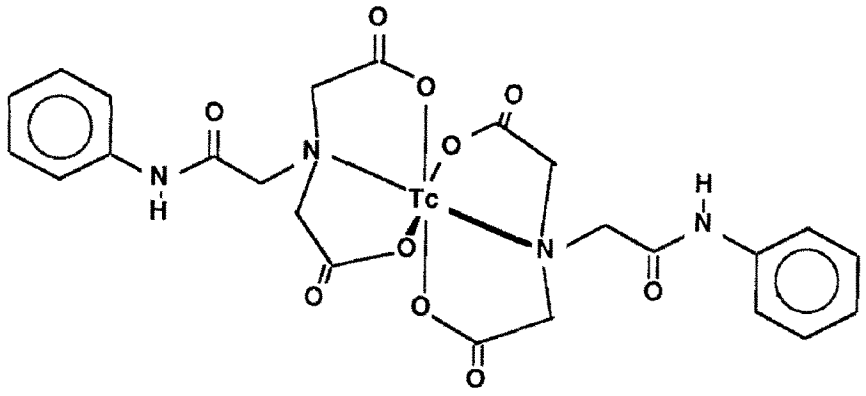

Fig. 15 Proposed structure of $[(HIDA)_2Tc]^-$. In the original lidocaine complex, methyl substituents are in ortho positions on the phenyl rings.

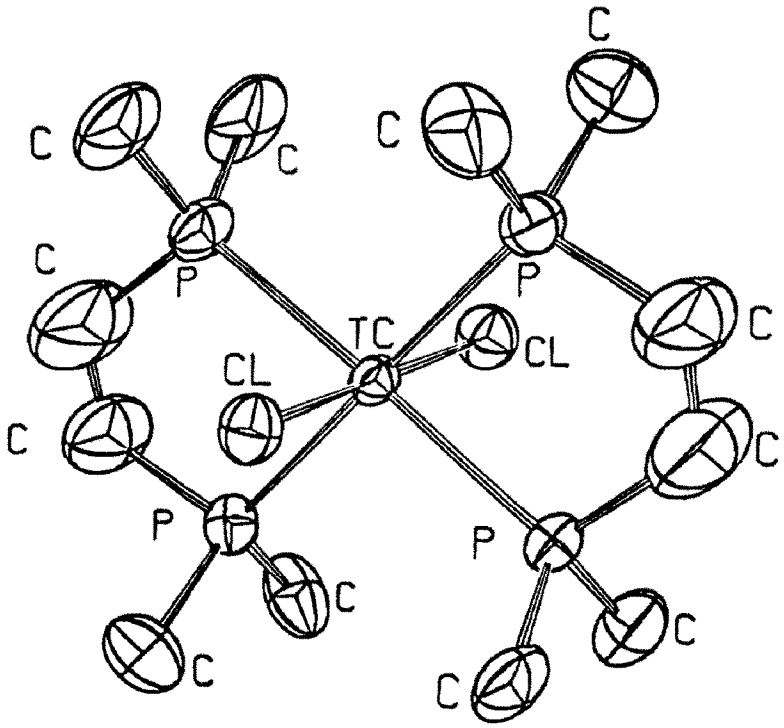

Fig. 16 Structure of the myocardial imaging agent *trans*-$[Cl_2(DMPE)_2Tc]^+$ [173].

complex bears analogies to the monomeric EDTA species discussed previously and that it contains a $[Tc{=}O]^{3+}$ core. Further HPLC studies [162] have shown that there are two anionic components, which can be interconverted by changes in the pH and chloride concentration. This would be consistent with a labile site opposite the oxo ligand of a Tc(V) complex, which might be occupied by a water, hydroxide or chloride ligand or even an IDA carboxylate (analogous to the penicillamine complex). Moreover, since the product distribution is affected by the technetium concentration [99], it is possible that di- or oligomeric species are being formed, such as occur with EDTA and NTA.

Heart Imaging. The major use of imaging heart muscle (myocardium) is to aid in the detection of coronary artery disease. Imaging blood perfusion to the myocardium helps to differentiate between: a) normal blood flow, b) ischemia, a state in which blood flow is decreased usually as a result of the deposition of cholesteric plaque in the lining of the coronary arteries, and c) infarcted (dead) tissue, which occurs when the blood flow is insufficient to support viabililty in a segment of the myocardium.

Heart tissue tends to accumulate monovalent cations. Some radiotracers such as $^{81}Rb^{+}$ and $^{129}Cs^{+}$ appear to follow potassium ion, which is essential for normal function of heart muscle, and are taken in through the Na/K ATPase pump. Other cationic species such as ^{131}I-labeled ammonium salts also accumulate in the myocardium, but these are sufficiently different from K^{+} that it is unlikely they are processed by the Na/K pump [6]. The isotope ^{201}Tl is the most widely used myocardial imaging agent [163], but has a relatively low and somewhat broad γ-emission spectrum, which leads to diffuse focusing and consequent loss of resolution and contrast in the image [164]. Owing to the stability of Tl^{+} and its chemical similarity to K^{+}, it has been proposed that its accumulation in heart muscle is due to its ability to mimic K^{+}. Consistent with this, Tl^{+} has been shown to activate the Na/K ATPase system. However, it is possible that heart cells have relatively nonselective receptors for monocations, including Tl^{+}. For these reasons, there has recently been considerable interest in the preparation and evaluation of cationic complexes of ^{99m}Tc as potential myocardial imaging agents [165 ,166 ,167 ,168,169,170,171,

,172 ,173]. Deutsch and coworkers have recently surveyed a number of Tc(III) complexes of the general type *trans*-$[X_2(di)Tc]^+$ (where di = a diarsine or diphosphine ligands) as to their uptake by myocardial tissue. Initially, these compounds were prepared by combination of the ligand with $K_2[TcCl_6]$ [174]. The synthesis of these agents can also be accomplished by reaction of the ligand with $[n\text{-}Bu_4N][OCl_4Tc]$ in HCl/ethanol, from $[OCl_4Tc]^-$ generated *in* situ from $[TcO_4]^-$ or directly from $[TcO_4]^-$ in an acidic water/ethanol mixture. The presence of HCl is essential for removal of the oxo ligands, since in its absence the reaction with o-phenylenebis(dimethylarsine) (diars) produces *trans*-$[O_2(diars)_2Tc]^+$. The ligand also presumably serves as the reductant and may be oxidized by transfer of oxygen from the $[TcO_4]^-$.

An x-ray structure determination of *trans*-$[Cl_2(DMPE)_2Tc]^+$ (where DMPE = 1,2-bis(dimethylphosphino)ethane), the most successful of these as a myocardial imaging agent, shows a typical octahedral geometry with the chlorides *trans* to one another and the phosphorous atoms occupying the equatorial coordination sites (see Figure 16). HPLC of preparations of this complex revealed the presence of several impurities including the pertechnetate starting material--at least two of which are cationic complexes. Infrared analysis showed one to be the Tc(V) complex *trans*-$[O_2(DMPE)_2Tc]^+$, which is protonated to *trans*-$[O(OH)(DMPE)_2Tc]^+$ in strong acid with a K_a of 6.3. The Tc(III) compound undergoes a reversible one-electron reduction to *trans*-$[Cl_2(DMPE)_2Tc]^0$ at 0.1 V in DMF. The final cationic compound present in these reaction mixtures proved to be $[(DMPE)_3Tc]^+$, which was characterized by elemental analysis, ^{31}P-NMR and EXAFS, which revealed the Tc-P distances to be 2.40 Å. The presence of Tc(VII), Tc(V), Tc(III) and Tc(I) complexes in the same reaction mixture illustrates how subtle ligand, pH and reducing environmental effects can alter the technetium oxidation and coordination states. HPLC separation of the various ^{99m}Tc-components, which were identified by comparison with structurally characterized samples prepared with ^{99}Tc, provided for the evaluation of the biodistribution of the individual complexes.

While the *trans*-$[Cl_2(DMPE)_2Tc]^+$ provided excellent images of the heart in test animals, the results in humans were of

insufficient quality to warrant its use clinically. Interestingly, the rhenium analog *trans*-$[Cl_2(DMPE)_2Re]^+$, showed better heart localization and less liver uptake in rats. Since the structures of two ions are essentially identical, the variations in their biodistributions must be due to differences in reactivity. Since the reduction potential of the technetium complex is 190 mV more positive than that of the corresponding rhenium species, it is more likely to be reduced *in vivo*. This decreases the availability of the monocationic complex and produces the neutral Tc(II) complex, which exhibits enhanced uptake by the liver. Modifications of the ligand system which would lessen its π-acceptor abilities may sufficiently stabilize the Tc(III) species so as to render a clinically useful analog [175].

Hexakisisonitrile complexes of Tc(I) constitute class of monovalent cations that exhibit good heart localization and are likely to be used clinically. Complexes of the type, $[Tc(CNR)_6]^+$ (R=alkyl), were first prepared by ligand exchange onto ^{99m}Tc-glucoheptonate or from $[^{99}Tc(SC(NH_2)_6]^{3+}$ [77]. A more direct synthesis from $[^{99m}TcO_4]^-$ has been effected by reduction with Na_2SO_4 in the presence of the isonitrile ligand. These complexes are stable in solution and undergo oxidation to Tc(II) only in the presence of strong oxidants (E^o = 1.0 - 1.1 V). The *tert*-butyl isonitrile complex has been shown to accumulate well in the normal myocardium of both animals and humans in relation to the regional myocardial blood flow [176 . HPLC has demonstrated that the metabolism of these complexes is responsible in part for the time evolution of their biodistribution and initial results suggest musole uptake to be receptor mediated.

Imaging of myocardial infarcts is often exhibited by bone-imaging agents to a degree that generally parallels their localization in bone [177]. The calcium concentration in the relaxed normal myocardium cells is low (10^{-7} M), while that in the extracellular fluid and blood is much higher (10^{-3} M). When injured, these cells can no longer maintain this concentration gradient and extracellular calcium diffuses into the cells. Coupled with this is the availability of phosphate (from ATP, ADP, etc.) in infarcted cells, which leads to the deposition of amorphous calcium phosphate, crystalline hydroxy apatite, and

calcium complexed with myofibrils and other macromolecules. In infarcts induced by isoproterenol the maximum calcium concentration is reached after 4-8 hrs [178]. Since their accumulation is tied to the mechanism of calcium deposition, bone imaging agents show a more pronounced uptake 6-8 hr after necrosis had been initiated in animal models [179]. Consequently, these agents are more useful for imaging old infarcts (2-3 days) in the clinical setting than new ones (1 day). Of the bone-imaging agents the pyrophosphate complex has proven to be best for heart-imaging [180].

Both ^{99m}Tc-gluconate and ^{99m}Tc-glucoheptonate show significant accumulation in the infarcted myocardium of animal models and humans, with good quality infarct images being obtained any time within the first day of the infarction [181]. Their mechanism of localization is probably not associated with calcium deposition, but rather with cell permeability. Altered cell permeability, which would allow these agents to enter the cell and bind to tissue proteins, is expected to occur shortly after occlusion of blood flow has occurred. The time of maximum uptake for these radiopharmaceuticals in the lesion is much earlier than for the bone agents.

Imaging with ^{99m}Tc-Labeled Blood Cells. In assessing abnormalities of the cardiac chambers or circulatory system, visualization of the cardiovascular blood flow provides an important diagnostic aid. Ideal imaging agents for this purpose are retained by the blood in the intravascular space and are not easily secreted by the liver or kidneys. The incorporation of ^{99m}Tc into red blood cells has provided a nearly ideal blood pool imaging agent and paved the way for enormous growth in cardiovascular nuclear medicine [182].

Since erythrocytes are abundant, easily separated from other blood components, stable to mild mechanical or chemical manipulation, have less stringent nutritional requirements and have a variety of transmembrane transport systems, they are relatively easy to label with radionuclides. Highly efficient ($\geq$95%) procedures are now available [183], which employ a pretreatment with Sn(II) in the presence of citrate, glucoheptonate or other anionic oxygen ligands. While the labelling mechanism is not

clearly understood, during the pretreatment it is thought that the complexed stannous ion diffuses into the cell and becomes bound to a cellular component. Pertechnetate ion is then added and diffuses freely in and out of the cells, but upon encountering Sn(II) within the cell is reduced. Intracellular coordination then occurs to fix the Tc primarily to the β-chain of hemoglobin [184 ,185]. A widely used kit devised to label 4 mL of patient blood contains: 2 μg Sn(II), 3.67 mg sodium citrate, 5.5 mg dextrose and 0.11 mg NaCl [186]. Following a 5 min incubation period with the Sn(II), an aliquot of the packed cells is added to the generator ^{99m}Tc-eluant and incubation continued for another 10 min.

The relative amounts of Tc and Sn are critical. Since an excess of Sn(II) causes the extracellular $[TcO_4]^-$ to be reduced and so prevented from entering the cells, EDTA is added and the cells packed by centrifugation to hold the unreacted Sn(II) in the plasma. A portion of the packed cells is then separated and added to the $[^{99m}TcO_4]^-$. Alternatively, the excess Sn(II) can be removed by oxidation to Sn(IV) by the addition of NaOCl followed by EDTA, which serves to lower the oxidation potential of Sn(II). A pertechnetate concentration exceeding the reducing capacity of the Sn(II) results in the presence of free $[TcO_4]^-$. Approximately 10-30 mCi of ^{99m}Tc are used in a typical study and a labeling efficiency of 95-98% can be obtained with eluant solutions containing up to 10^{14} Tc atoms. In order to attain both the right ^{99m}Tc activity and total pertechnetate concentration, time control must be exerted over the generator elutions. For example, an eluate of 10 mCi ^{99m}Tc-activity contains 10^{13} Tc atoms when eluted after a generator resting period of 3 hours, but this rises to 10^{14} atoms after 50 hours [187].

Despite the efficiency and high reproducibility of ^{99m}Tc-erythrocytes prepared in this manner, the patient must be phlebotomized and the blood manipulated externally. Consequently, clinicians often prefer an *in vivo* labelling method that utilizes similar reagents [188], but is accomplished by sequential injections into the patient, who serves as the reaction vessel. Owing to the dilute conditions and presence of other oxidizing agents, it is unlikely that the Sn(II) alone reduces the pertechnetate. It has been proposed that the tin activates a redox

mechanism in the erythrocytes and the choroid plexus resulting in *in situ* reduction and retention of ^{99m}Tc at these sites [189]. A combination of both methods has been developed which involves *in vivo* introduction of the tin followed by *in vitro* mixing of small portions of the blood with $[^{99m}TcO_4]^-$ through an indwelling intravenous catheter [190].

Erythrocytes labeled with ^{99m}Tc have diverse clinical applications. They are primarily used in the evaluation of the cardiovascular system [191] and detection of gastrointestinal bleeding [192], but have also been applied to the measurement of cerebral blood flow and the assessment of the vascularization of brain tumors. More recently, they have begun to play an important role in the evaluation of hemangiomas, which are benign tumors of blood vessels containing a large volume of blood [193].

The labeling of other blood cell components, such as leukocytes [194] and platelets, with ^{99m}Tc would be highly desirable, but stable products have eluded investigators. Tagged leukocytes would be helpful in identifying sites of internal infections and infarcts. ^{99m}Tc-platelets could be employed to image blood thrombi and possibly platelet deposition on the plaque of atherosclerosed blood vessels [195]; however, the half-life of ^{99m}Tc may be to short for the latter.

Splenic Imaging. The spleen is particularly susceptible to damage by internal trauma, which may result in hematoma, rupture and severe hemorrhage. Consequently, visualization of the spleen's morphology is a valuable diagnostic aid. Scans of the region of the spleen are also helpful in determining if a splenectomy was complete or if the patient is asplenic [196]. Among the spleen's functions is to eliminate damaged or aged erythrocytes from the blood by means of its uniquely narrow and tortuous circulation. Red blood cells that have been tagged with ^{99m}Tc and subjected to heat damage by incubation at 49.5 $^{\circ}$C for 15 min [197] are insufficiently flexible to squeeze through the smaller pores and fenestrations in the spleen's endothelial cells. The trapped cells are then phagocytized and permanently removed from circulation. Since damaged erythrocytes are taken up exclusively by the spleen, they constitute an excellent vehicle for splenic imaging.

Since both the spleen and liver filter out small particles from the blood, each can be imaged with colloids incorporating ^{99m}Tc. Presently the most important particulate employed for this purpose is the ^{99m}Tc-sulfur colloid, which is usually prepared by the reaction of $[^{99m}TcO_4]^-$ with thiosulfate. In acid solution $[S_2O_3]^{2-}$ disproportionates to produce SO_2, elemental sulfur and water. The reaction is usually carried out around 97 ^oC to enhance the rate. While the disproportionation to produce H_2S is not favored thermodynamically at 25 ^oC, analogy to the chemistry of Re [198] and the production of a similar colloid with H_2S lead to the belief that a product incorporating Tc_2S_7 is formed from H_2S generated during the reaction. Since the amount of Tc employed is so low, conventional methods of analysis have not revealed the structure of the colloid [199]. Thiosulfate is also capable of reducing $[TcO_4]^-$, which raises the possibilty that the agent is comprised of a reduced Tc complex adsorbed on the surface, or incorporated into an elemental sulfur colloid. When gelatin is added as a stabilizer, the colloid generated has a fairly narrow size distribution, with 80% of the particles between 0.1 and 1.0 μm [200]. Direct reaction with H_2S is not as convenient, but results in a nearly uniform size with ~90% of the particles having a diameter of 0.09 $\pm$ 0.01 μm [201]. Water dispersions of ^{99m}Tc-sulfur colloid taken orally provide images of the esophagogus, which have yielded useful data in the diagnosis and follow-up of many esophageal diseases [202].

Lymphoscintigraphy. The lymphatic system is responsible for the extraction of small particles from the interstitial space, with colloids in the range of 1 to 10 nm being most efficiently eliminated. It is the purpose of lymphatics to stem and contain infection and neoplastic growth through isolation and phagocytosis of foreign bodies; however, in performing this function they can also serve as a primary pathway for the dissemination of invading cells. Lymphoscintigraphy is the imaging of the lymph nodes after the interstitial, intraperitoneal, or intralymphatic injection of a radiocolloid [203]. Colloids incorporating ^{198}Au are uniformly small (3 - 5 nm) and exhibit the best lymphatic uptake, but generate an unacceptably high radiation dose to the patient. While ^{99m}Tc-sulfur colloids are used for lymphatic imaging, an antimony sulfide colloid (Tc-Sb_2S_3) incorporating ^{99m}Tc gives a narrow size

distribution in the range of 10 nm and is the agent of choice for most lymph node imaging [204 ,205 ,206 ,207]. Lymphoscintigraphy is partioularly useful in the management of several forms of cancer [208], especially that of the breast [209], and is also helpful in diagnosing hereditary lymphedema (Milroy's disease), demarcating lymphatic pathways following surgery, and in evaluating lymphatic drainage from particular organs [210].

Lung Imaging. All ^{99m}Tc-lung imaging agents are microparticulates which are injected intravenously. They are of sufficient size (› 10 μm) so that, after reaching the right side of the heart, they are pumped into the pulmonary artery and then become trapped in the arteriolar capillary bed of the lung. In effect, these radiopharmaceuticals image blood flow into the first set of capillaries encountered that are sufficiently small to seine them from the blood. While these agents do block capillary blood flow, this is a marginal effect and their use is deemed safe for routine application [8]. The most popular ^{99m}Tc-lung imaging agent consists of microspheres of denatured human serum albumin, which are available in kit form and are labeled by stannous reduction [211]. Other particulates used are macroaggregrated albumin [212] and iron hydroxide [213].

In providing both static images of the lung and a measurement of lung perfusion, lung scans are helpful in diagnosing pulmonary thromboembolisms. While nonspecific, pulmonary imaging with ^{99m}Tc-microspheres can yield the earliest clue for the correct diagnosis of fat embolism, air embolism, contusion or laceration. A quantitative method for measuring increased pulmonary capillary permeability, which results in edema arising from the leakage of water and protein into the pulmonary interstitial space following some microvascular injury, has been developed using ^{99m}Tc-labeled human serum albumin (HSA, see below). This is based on the migration of ^{99m}Tc-HSA from the capillaries into the extravascular space in the pulmonary region, which increases the activity in the lung relative to that in the blood measured at the heart. Following the rate of change of this ratio with time allows for the early diagnosis of acute respiratory distress syndrome and accurately differentiates this condition from pneumonia or cardiogenic pulmonary edema [214].

^{99m}Tc-Labeled Proteins and Macromolecules. Radiolabeled human serum albumin (HSA) is useful in determining blood pool volume, cardiac parameters and other measurements involving the plasma [215]. While a number of methods have been tried, the most efficient labeling of HSA with $[^{99m}TcO_4]^-$ has been achieved using stannous reduction in the presence of the protein at low pH. DTPA or tartrate [216] are commonly used as a chelating agent for the Sn(II), which helps to avoid the formation of Sn-Tc colloids [217]. Sulfhydryl groups on the surface of the protein are thought to provide binding sites for the metal [218]. Neither the oxidation state nor the coordination geometry of the bound technetium has been characterized with certainty [219]. Quality control of ^{99m}Tc-HSA adducts is a problem, since a variety of free and colloidal technetium side products are formed together with HSA aggregates and weakly bound (ion-paired) technetium [220]. While suitable chromatographic separations have been developed to yield good quality ^{99m}Tc-HSA, these make the preparative procedure more involved and aggravate the difficulty of injecting a pyrogen-free radiopharmaceutical. The use of modern resonance Raman spectroscopic techniques promises to be useful in determing the nature of technetium coordination sites on proteins even at metal concentrations approaching the no carrier added level [221].

An agent capable of imaging intravascular blood clots would be of tremendous utility in the diagnosis of thromboembolic disorders. Indeed, several attempts have been made to adapt the stannous reduction procedure to label fibrinogen [222], urokinase [223], and streptokinase [224]. Unfortunately, none of these have reached the level of clinical utility. Nevertheless, the general approach of labeling proteins involved in clotting or dissolution of thromboses remains a logical path to follow.

Brain Scintigraphy. While CAT scans have become the major imaging tool in the evaluation of most brain lesions, expense and availability often dictate that radioscintigraphy be performed instead. Indeed, in cases where an assessment of blood perfusion to the brain is needed, radionuclide brain scintigraphy is often essential [225]. The advent of SPECT instruments, which are particularly useful for head scans, has intensified the search for ^{99m}Tc-agents which effectively cross the blood-brain barrier. The

present radiopharmaceuticals of choice, ^{99m}Tc-DTPA or glucoheptonate (discussed under renal agents) have both been shown to provide higher sensitivity than $[^{99m}TcO_4]^-$, but enter the brain only when the barrier membranes have been damaged. Injections of these agents can furnish several kinds of information. First, blood flow in the carotid and cerebral arteries can be immediately visualized and then followed by a blood pool study. Static imaging of the brain is begun no sooner than 1 hr after the injection, followed by later views, if deemed necessary. Epileptic seizures often cause increased blood flow in the region of the discharge, so that this may appear as an area of increased radioactivity. In cases of head trauma the dynamic phase of the radioscintigraphy may help distinguish between subdural and epidural hematomas [225].

The development of brain agents is hampered by the difficulty of overcoming the "blood-brain barrier", which efficiently excludes large or foreign materials from the cerebrospinal fluid. Small, diffusable radiotracers have been most successful in penetrating cerebrospinal membranes and the agents presently in use are hydrophilic anions. However, increasing the lipophilicity of the ^{99m}Tc-complex (as measured by the octanol/water partition coefficient) by enlarging the size of the organic groups on the ligands appears to increase their membrane permeability and ability to diffuse across the blood-brain barrier [226].

A series of mono-oxo Tc(V) complexes with derivatives of 3,3′-(1,3-propanediyl diimino)bis(3-methyl-2-butanone oxime) (PnAO) have been synthesized by the stannous reduction of $[TcO_4]^-$ in the presence of excess ligand. These neutral square-pyramidal complexes exhibit significant lipophilicity and diffuse well across the blood-brain barrier. Upon coordination the PnAO ligand loses two amine protons and a single oxime proton, with the remaining oxime proton being strongly hydrogen bonded between the two oxime oxygens. Substituents on the PnAO ligand can be oriented toward or away from the apical oxygen and so give rise to diastereomers [227]. The first of these complexes to be used clinically is the hexamethyl derivative (HM-PAO) (see Figure 18), which shows high brain uptake and retention and good discrimination between the grey and white regions of the brain [228].

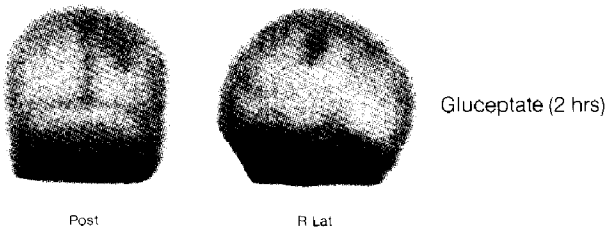

Fig. 17 Posterior and right lateral views of the brain revealing lesion in right posterior quadrant. Images taken 2 hr. after injection with ^{99m}Tc-glucoheptonate. (*Courtesy, DuPont, NEN Products*).

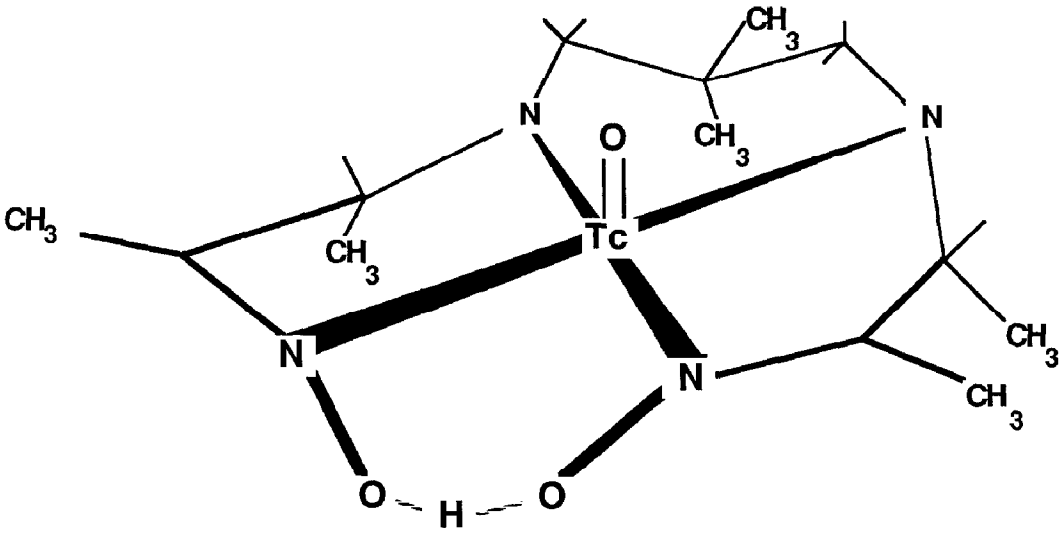

Fig. 18 Diagramatic representation of the essential features of one of the diastereomers of [O(HM-PAO)Tc] used for brain imaging.

An interesting approach to the systematic development of heart and brain agents takes advantage of the vast array of benzene derivatives, which can be incorporated into dibenzene technetium complexes of the type, $[\emptyset_2Tc]^+$ [229]. These complexes are conveniently prepared by the reaction of the benzene ligand with $[TcO_4]^-$ in the presence of Al as a reductant and $AlCl_3$ as a catalyst so that the size and lipophilicity of the product can be varied almost at will [230].

Reproductive Organs. Microspheres made from human albumin tagged with ^{99m}Tc have recently been used to illustrate the migration of nonmotile particulates up the vagina through the uterus and fallopian tubes into the peritoneal cavity and ovaries [231]. Pertechnate has been shown to be useful in dynamic and static imaging of blood perfusion of the scrotum and testes to differentiate between inflammatory disease and torsion of the testis [232]. Since the scan can be completed in 15 minutes and inflammation is accompanied by an increase in blood flow, while torsion is associated with decreased perfusion, a rapid differential diagnosis is often possible without exploratory surgery.

Thyroid and Parathyroid Imaging. Although cancer of the thyroid is relatively uncommon, the appearance of benign nodules on the thyroid occurs 30 times more frequently. Since the nature of an intrathyroidal nodule is not readily discerned by patient history or physical examination and exploratory surgery is neither practical nor justifiable in the majority of cases, the functional information derived from radioscintigraphy has become a central diagnostic factor [233]. Owing to the thyroid's metabolism of iodine to form thyroxine, primary thyroid cancers accumulate ^{131}I, but less avidly than normal thyroid tissue. Cancers metastasized from the thyroid also exhibit uptake of radioiodine, but the use of ^{131}I produces a relatively high radiation dose to the thyroid and its γ-ray energy is higher than is desirable for efficient imaging. In addition to I^-, the thyroid traps certain monoanions including: Br^-, $[ClO_4]^-$, $[MnO_4]^-$, $[TcO_4]^-$, and $[ReO_4]^-$; however, these are not metabolized and are eventually released. Presently, $[^{99m}TcO_4]^-$ is the most commonly used tracer for thyroid imaging. The presence of a "cold nodule" on the thyroid imaged with $[^{99m}TcO_4]^-$ is not in

itself diagnostic for a malignancy; however, a suggestive clinical history and the presence of other cold defects or nodules increases the likelihood. A low percentage of nodules appearing "hot" on a ^{99m}Tc-scan also prove to be malignant. Metatastases from the thyroid are most easily visualized with $[^{99m}TcO_4]^-$ and such scans are helpful in determining the spread of the disease and in planning for surgery.

The four relatively small (~40 mg each) parathyroid glands are responsible for the secretion of the parathyroid hormone, which assists in the regulation of calcium levels, and are situated adjacent to the thyroid. Consequently, they are usually difficult to distinguish from the thyroid and the background from the thyroid must be digitally subtracted using a double-radiotracer technique. In a typical method, $[^{99m}TcO_4]^-$ is injected intravenously, a thyroid scan taken, and the data stored on a computer. This is followed by an injection of $^{201}Tl^+$ and a scan of its distribution in the region of the thyroid. The background ^{99m}Tc image is then subtracted from the ^{201}Tl picture to yield a view of ^{201}Tl uptake by the parathyroids alone. Enhanced ^{201}Tl uptake provides evidence for parathyroid hyperplasia, adenomas or carcinomas [234].

Oncological Applications.

A number of attempts have been made to design ^{99m}Tc-radioscintigraphic agents that would be specific for certain types of tumor tissue. Unfortunately, only very limited success has been acheived in attaining stable, truly tumor-specific drugs. Most radiopharmaceuticals used in cancer diagnosis are organ-specific agents, such as those already discussed. Owing to their high sensitivity and ability to image function as well as structure, ^{99m}Tc-radiopharmaceuticals play a critical role in the detection of cancer and assessment of the stage of the disease. Depending on the nature of the function imaged, a tumor may appear as a "cold" or a "hot" area on the scintigraph. For example, neoplasms generally appear as regions of decreased radioactivity in the thyroid imaged with $[^{99m}TcO_4]^-$ or in the reticuloendothelial system of the liver imaged with ^{99m}Tc-sulfur colloid, since tumors in these organs represent a decrease in the normal function. On the other hand, brain tumors visualized with $[^{99m}TcO_4]^-$ or bone tumors detected with ^{99m}Tc-phosphonates are seen as increased areas of

radioactivity. This is probably due to the relatively higher metabolism, increased blood perfusion, and greater degree of membrane permeability usually exhibited by tumor tissue [235 , 236]. Direct measurement of tumor volume by radionuclide methods has recently become possible with tomographic cameras [237].

The detection of cancer metastases occurring in bone by x-radiography or enzyme tests is often unreliable. On the other hand, micrometastases can be visualized by ^{99m}Tc-bone agents several months before they are visible by x-ray and are detected in 30-50% of patients with normal radiographic studies in the same region [238]. Bone scanning has become an important use of ^{99m}Tc-agents in the management of breast cancer [239]. Scans are normally performed preoperatively in patients with clinical findings suspicious for breast cancer, and metastases to the skeleton are detected in about 10% of these cases [240]. Determining that the stage of the disease has advanced considerably spares some of these patients from aggressive surgical procedures. Serial bone scanning in patients with known metastases is valuable in determining a patient's response to therapy and in localizing lesions for biopsy. Bone-imaging agents have also proved useful for imaging soft tissue neoplasms of the musculoskeletal system, possibly as a result of calcification arising from damaged cells [241]. Calcification has been reported in up to 50% of patients with neuroblastoma; however, it appears that calcification may be found in almost every neuroblastoma and that it occurs in living tumor cells as well as in areas of necrosis. Uptake is believed to be related to calcium metabolism, with the rate of calcium metabolism (rather than the total amount of calcium present in the tumor) being the most important factor in determining uptake [242].

Surgical removal of the lymphatics draining a cancerous region often accompanies the excision of some tumors [243]; however, in the absence of lymphscintigraphy, it is not always obvious as to which lymph nodes are involved. When the lymphatics are not removed, tracing the lymphatic drainage of a tumor is also important in directing radiation therapy to the appropriate lymph nodes to prevent spread of the disease [209]. Identifying the degree of lymphatic involvement is often possible on scans

following the injection of ^{99m}Tc-sulfur or antimony-sulfur colloids into the affected region. Tumors studding peritoneal surfaces result in a marked exudation of fluid (ascites), which tends to accumulate as a result of ascitic tumor cells blocking lymphatic channels [203]. Lymphoscintigraphy readily reflects the ability of the regional lymph channels to drain the area and provides an indication of the severity of the disease. Extensive lymphatic involvement in cases of breast cancer establishes a grave prognosis and the futility of any attempt at radical surgery [209]. Chemotherapeutic agents are sometimes administered through a transabdominal infusion catheter to treat metastatic tumors. The introduction of ^{99m}Tc-HSA into the peritoneal cavity provides a means of studying fluid distribution as well as identifying the catheter position to insure proper distribution of the anticancer drug [244]. Scintigraphy with $[^{99m}TcO_4]^-$ has been shown to have about the same degree of accuracy in diagnosing breast abnormalities and provides a good complement to x-ray (mammography) techniques [245].

Probably as a result of their increased metabolism, neoplasms typically show a high affinity for porphyrins and hematoporphyrins. For the most part, ^{99m}Tc-labeled porphyrin derivatives have yielded inconclusive results in delineating tumors. However, one recent study showed that a ^{99m}Tc-hematoporphyrin derivative localized in both malignant and benign tumors [246]. Tumors also tend to exhibit a high requirement for nucleotides. Several lines of human tumor cells in culture allow permeation of low levels of adenine nucleotides thorugh their plasma membranes. In contrast, untransformed cells generally do not incorporate adenine nucleotides into their cellular pools without prior degradation to adenosine. Biodistribution studies demonstrated that ^{99m}Tc-Ap_4A accumulated preferentially in RT-24 tumors implanted in rats. This agent also concentrated in V2 carcinoma implanted in rabbits sufficiently to visualize the tumor by *in vivo* imaging. Tumor-to-muscle ratios with ^{99m}Tc-Ap_4A or ^{99m}Tc-ATP were higher than those the widely used tumor imaging agent, ^{67}Ga-citrate [247].

Stemming from the ability of some antibiotics to cure certain types of cancers and arrest others, a number of attempts have been made to label tumor-localizing antibiotics with ^{99m}Tc in order to

produce a tumor-specific agent. In particular, tetracyclines and bleomycin show some degree of tumor concentration; however, this may to be due to a passive process rather than active tumor uptake or binding to specific receptor sites on the tumor [236]. Bleomycin is the name given to a group of structurally similar glycopeptide antibiotics with molecular weights around 1400 produced by a strain of Streptomyces verticillus [248 ,249]. Poorly characterized ^{99m}Tc adducts have shown some sensitivity in detecting abdominal tumors,[250 ,251] but their low stability is a major problem. The antibiotic ionophore lasolocid A, which exhibits a tendency to enter tumor cells, forms a 2:1 complex with Tc containing a $[Tc{\equiv}O]^{3+}$ core to which the antibiotic is coordinated through its salicylate moiety. The exact nature of the coordination remains to be established as does its efficacy as an imaging agent [252].

Mammalian immunoglobin G (IgG) has been labeled by reduction of $[^{99m}TcO_4]^-$ with HCl or $SnCl_2$ and radiochemical purity determined by immobilization of the product on protein A from S. aureus [253]. An area of intense investigation is the radiolabelling of tumor-specific monoclonal antibodies that recognize tumor-associated antigens [254]. Since they are carried by the blood stream, individual antibodies are transported throughout the body bypassing normal tissues but attaching to tumor antigens. Over time, a large concentration of antibodies may attach to the tumor. However, their concentration in the tumor is highly dependent on their ability to arrive at the antigen site and so depends on variables such as tumor perfusion and permeability as well as the accessibility of the antigen. Appropriate radiolabelling of these antibodies without destroying their specificity could make available highly selective tumor-imaging agents. A host of tumor associated antigens have now been discovered and many monoclonal antibodies can be produced in large amounts [255]. Results obtained with polyclonal antibodies against the carcino-embryonic antigen (CEA), human chorionic gonadotropin (HCG), α-fetoprotein, kidney carcinoma and ferritin revealed that the amount of radiolabeled antibody which localized in the tumor was low compared with that in the blood and other organs [256]. Fragments of IgG designated as Fab and $F(ab')_2$ have also been used successfully to image human tumors [257]. The high background arising from

antibodies remaining in the blood and other organs, especially the liver, has necessitated the use of double radionuclide techniques often employing $[^{99m}TcO_4]^-$ to subtract out the background [258].

Unfortunately, the relatively short half-life of ^{99m}Tc and the low stability of the protein adducts so far prepared has limited its utility in labeling monoclonal antibodies. For the latter reason, attempts have been made to covalently attach strong chelating groups to the protein that would hold the metal securely. One approach that effectively links DTPA to proteins through an efficient coupling involving the DTPA bicyclic anhydride holds promise in this regard [259 ,260]. In this simple procedure a few microliters of protein solution are added to the dried anhydride and the mixture agitated for 1 min. Efficiently and effectively linking ^{99m}Tc to antibody proteins may well yield a useful family diagnostic tools for diagnosing cancers.

Concluding Comments.

It is not surprising that ^{99m}Tc-radiopharmaceuticals have been most successful at imaging organs whose function involves the elimination of alien or undesired materials. Since technetium is foreign to natural systems, it is indeed difficult to chemically disguise it so that it could be readily accepted into metabolic processes. Only in the case of the bone have researchers been clever or lucky enough to develop an agent, which is highly selective by virtue of its incorporation directly into the specific metabolism of the target tissue. For a number of organs no clinically useful ^{99m}Tc-radioscintigraphic agents are yet available. These include: the heart and other muscles, the prostate gland, endocrine glands such as the pancreas, adrenals, and pituitary, and gastrointestinal lesions such as ulcers. Indeed, no organ is imaged with such quality that improvement should not be sought.

Effectively employing ^{99m}Tc to visualize intravascular thromboses would provide an enormously useful diagnostic aid. Perhaps further advantage can be taken of technetium's ability to bind firmly to Ca^{2+} sites by extending its binding to calcium binding proteins, especially those which are associated with the

formation of blood clots. The impending availability of significant quantities of useful proteins derived from biogenetic technologies may play an important role in these endeavors. Alternatively, simpler polypeptide complexes involving γ-carboxyglutamates, which are frequently used to bind Ca^{2+} in proteins and polypeptides [261], might yield promising agents.

Efforts at firmly attaching ^{99m}Tc to biologically important molecules have been somewhat hampered by the instability of Tc-N bonds involving the metal in a mid oxidation state. Technetium(IV) and (V) compounds with monodentate nitrogen ligands readily hydrolyze in aqueous solution, and most nitrogen ligands are insufficient as π-acids to stabilize the lower oxidation states. One outstanding exception to this is the extraordinary stability of the Tc-N bonds in trans-$[(NO)(H_2O)(NH_3)_4Tc]^{2+}$ and the corresponding complex with Tc(II) [262]. In these complexes the nitrosyl group delocalizes sufficient π-electron density away from the Tc that the σ-bonds to the ammine nitrogens are greatly stabilized. As a result, these complexes are very slow to undergo substitution. The use of other good π-acceptor nitrogen ligands may make available new synthetic starting materials for the formation of stable complexes with amino acids, nucleotides and their polymers. The recently available nitrido complexes also offer promise in labelling these biomolecules.

Despite the wide range of synthetic reactions now documented for technetium complexes, relatively little is known about the processes by which they occur. Of the few that have been investigated, somewhat surprising mechanisms have been uncovered. Owing to the centrality of Tc in the transition elements, it may be abundantly versatile in mechanistic processes, with subtle changes in the ligands opening a variety of reaction pathways. Its tendency to form oxo-bridged polymers and the importance of ^{99m}Tc-colloids in diagnostic imaging further suggests that mechanisms of dimer and oligomer formation might be a worthwhile area for study.

At the present time only the broad outlines of technetium chemistry have taken shape, but steady progress is now underway. Expanding our insignt into the synthesis and reactivity of technetium compounds and joining this with a knowledge of the

physiological functions of organs to design imaginative, new ^{99m}Tc-radiopharmaceuticals presents a challenging prospect to the modern coordination chemist.

Acknowledgement.

Work in the author's laboratory has been supported by PHS grants GM-26390 and CA-24344 and a grant from the American Cancer Society (Massachusetts Division).

References

1. P. Richards, W.D. Tucker, S.C. Srivastava, S.C., *Int. J. Appl. Radiat. Isot.*, **33** (1981) 793-799.

2. A. Davison, A.G. Jones, A.G., *Int. J. Appl. Radiat. Isot.*, **33** (1982) 875-881. "The Chemistry of Tc(V)."

3. A.G. Jones, A. Davison, *Int. J. Appl. Radiat. Isot.*, **33** (1982) 867-874. "The Chemistry of Tc(I), II, III and IV."

4. K. Schwochau, *Radiochem. Acta*, **32** (1983) 139-152. "The Present Status of Technetium Chemistry."

5. E. Deutsch, K. Libson, K., *Comments in Inorg. Chem.*, **3** (1984) 83-103. "Recent Advances in Technetium Chemistry: Bridging Inorganic Chemistry and Nuclear Medicine."

6. E. Deutsch, K. Libson, S. Jurisson, L. Lindoy, *Prog. Inorg. Chem.*, **30** (1983) 75-139.

7. J.E. Turp, *Coord. Chem. Rev.*, **52** (1983) 241-247. "Technetium"

8. S.C. Srivastava, P. Richards, in "Radiotracers for Medical Applications", Rayudu, G.V.S., ed., CRC Series in Radiotracers in Biol. & Med., CRC Press, Boca Raton, FL, 1983, pp. 107-185.

9. M.J. Clarke, P.H. Fackler, *Structure and Bonding*, **50** (1982) 57-78. "The Chemistry of Technetium: Toward Improved Diagnostic Agents."

10. G. Bandoli, U. Mazzi, E. Roncari, E. Deutsch, *Coord. Chem. Rev.*, **44** (1982) 191. "Crystal Structures of Technetium Compounds"

11. G.J. Hine, J.A. Sorenson, in "Instrumentation in Nuclear Medicine", Academic Press, NY, 1974.

12. E. Deutsch, W.R. Heineman, J.P. Zodda, C.C. Williams, *Int. J. Appl. Radiat. Isot.*, **33** (1982) 843-848. "Preparation of no carrier added ^{99m}Tc complexes; determination of the total technetium content of ^{99}Mo/^{99m}Tc generator eluents."

13. M.D. Blaufox, L.M. Freeman, (eds.), "PDR for Radiology and Nuclear Medicine", Medical Economics Co., Oradell, N.J., 1976, pp. 3-5.

14. "Nuclear Medicine-Factors Influencing the Choice and Use of Radionucleotides in Diagnosis and Therapy", Report No. 70, Nat. Council on Rad. Prot. and Meas., Bethesda, MD 20814, 1982.

15. R.N. Beck, in "Nuclear Medicine", H. Wagner, ed., H-P Publishing, New York, 1975. "Instruments: Basic principles."

16. Available from Oak Ridge National Laboratory for $58/g of Tc.

17. V.K. Schwochau, *Z. Naturforsch*, **17a** (1972) 630.

18. A. Guest, C.J.L. Lock, *Can. J. Chem.*, **50** (1972) 1807-1810.

19. A. Guest, H.E. Howard-Lock, C.J.L. Lock., *J. Molec. Spect.*, **43** (1972) 273-281.

20. A. Davison, A.G. Jones, M.J. Abrams, *Inorg. Chem.*, **20** (1981) 4300-4302."New 2,2'-Bipyridine and 1,10-Phenanthroline Oxohalide Complexes of Tc(VII) and Tc(V)."

21. J. Binenboym, U. El-Gad, H. Selig, *Inorg. Chem.*, **13** (1974) 319-321.

22. E. E. Baran, *Spec. Let.*, **8** (1975) 599-603.

23. M.W. Billinghurst, S. Rempel, B.A. Westendorf, *J. ^{99m}Nucl. Med.*, **20** (1979) 138-143. "Radiation decomposition of ^{99m}Tc radiopharmaceuticals."

24. C.L. Rulfs, W.W. Meinke, *J. Am. Chem. Soc.*, **74**, (1952) 235.

25. L. Astheimer, K. Schwochau, K., *J. Inorg. Nucl. Chem.*, **38** (1976) 1131-1134.

26. K. Schwochau, L. Astheimer, J. Hauck, H.J. Schenk, *Angew. Chem. Int. Ed.*, **13**, (1974) 346-347.

27. L. Astheimer, J. Hauk, H.J. Schenk, K. Schwochau, K.; *J. Chem. Phys.*, **63** (1975) 1988-1991.

28. E. Deutsch, W.R. Heineman, R. Hurst, J.C. Sullivan, W. Mulac, G. Sheffield, *J. Chem. Soc., Chem. Commun.*, (1978) 1038-40.

29. A.G. Jones, C. Orvig, H.S. Trop, A. Davison, M.A. Davis, *J. Nucl. Med.*, **21**, (1980) 279-281. "A Survey of Reducing Agents for the Synthesis of $(Ph_4As)[O(C_2H_4S_2)_2Tc]$ from $[^{99}TcO_4]^-$ in Aqueous Solution."

30. M.R. Zalutsky, G.V.S. Rayudu, A.M. Friedman, *Int. J. Nucl. Med. Biol.*, **4**, (1977) 224-230. "The biological behavior of tin following administration of nine ^{99m}Tc-Sn complexes."

31. A. Kappas, M.D. Maines, *Science* **192**, (1976) 60. "Tin: A potent inducer of hemeoxygenase in kidney."

32. J. Steigman, E.V. Chin, N.A. Solomon, *J. Nucl. Med.* **20**, (1979) 766. "Scintiphotos in rabbits made with ^{99m}Tc preparations reduced by electrolysis and by $SnCl_2$."

33. E. Deutsch, *Proc. Natl. Acad. Sci. USA* **73** (1976) 4287.

34. J. Baldas, J. Boas, J. Bonnyman, M.F. Mackay, G.A. Williams. *Aust. J. Chem.*, **35**, (1982) 2413-2422. "Structural Studies of Tc Complexes. III. The crystal structure of tris[2-aminobenzenethiolato(2-)-**S,N**]Tc(VI): a trigonal-prismatic technetium geometry."

35. J. Baldas, J.F. Boas, J. Bonnyman, J.R. Pilbrow, G.A. Williams, *J. Am. Chem. Soc.* **107** (1985) 1886-1891. "ESR Study of Tris [2-aminobenzenethiolato(2-)-S,N]Tc(VI) and Re(VI) Chelates: Evidence for Molecular Aggregation in Solution."

36. U. Abram, R. Munze, R. Kirmse, J. Stach, *J. Nucl. Med. All. Sci.*, **29**, (1985), 185. "EPR investigations on Tc compounds."

37. D. W. Wester, D.H. White, F.W. Miller, R.T. Dean, *Inorg. Chem.*, **23**, (1984) 1501-1502. "Synthesis and Characterization of a Technetium Phosphite Complex: Hexakis(trimethyl phosphite)technetium(I) Tetraphenylborate."

38. M.J. Abrams, A. Davison, A.G. Jones, C. Costello, *Inorg. Chim. Acta*, **77**, (1983) L235-236. "Synthesis and Characterization of a New Tc(IV) Cation: Tris(acetylacetonato)technetium(IV) Tetrafluoroborate."

39. S.K. Shukla, *J. Chromat.*, **151**, (1978) 51-57. "Reduction of pertechnetate-99m ion by hydrochloric acid. I. Preparation of chromatographically pure ^{99m}Tc(IV)."

40. F.A. Cotton, A. Davison, V.W. Day, L.D. Gage, H.S. Trop, *Inorg. Chem.* **18**, (1979) 3024-3029. "Preparation and Structural Characterization of Salts of Oxotetrachlorotechnetium(V)."

41. R. W. Thomas, A. Davison, H.S. Trop, E. Deutsch, *Inorg. Chem.*, **19**, (1980) 2840-2842. "Preparation, Characterization, and Synthetic Utility of Oxotetrachlorotechnetate(V) Species $[OX_4Tc]^-$."

42. W. Preetz, G. Peters, *Z. Naturforsch.*, **35b**, (1980) 1355-1358. "Darstellung und Charakterisierung der Tetrabutylammoniumsalze der Tetrahalogenoxotechnetate(V), $[OCl_4Tc]^-$ and $[OBr_4Tc]^-$."

43. G. Peters, W. Preetz, *Z. Naturforsch.*, **36b**, (1981) 138-140. "Preparation and Characterization of Tetrabutylammonium Tetraiodooxotechnetate(V), (TBA)$[TcOI_4]$".

44. A.G. Jones, B.V. DePamphilis, A. Davison, *Inorg. Chem.* **20** (1981) 1617-1618. "Preparation and Crystal Structure of Tetraphenylarsonium Bis(2-mercaptoethanolato)oxotechnetate".

45. R.W. Thomas, G.W. Estes, E. Deutsch, *J. Am. Chem. Soc.*, **101**, (1979) 4581-4585. "Technetium Radiopharmaceutical Development. 1. Synthesis, Characterization and Structure of Dichloro[hydrotris(1-pyrazolyl)borato]oxotechnetium(V)."

46. S. Jurisson, L.F. Lindoy, K.P. Dancey, M. McPartlin, P.A. Tasker, D.K. Uppal, E. Deutsch, E., *Inorg. Chem.*, **23**, (1984) 227-231. "New Oxotechnetium(V) Complexes of N,N′-Ethylenebis(acetylacetone imine), N,N′-Ethylenebis(salicylideneamine), and o-Phenylenebis(salicylideneamine), X-ray Structures of $[TcO((sal)_2en)Cl]$ and $[TcO(H_2O)(acac_2en)]^+$."

47. P.H. Fackler, M.E. Kastner, M.J. Clarke, *Inorg. Chem.*, **23**, (1984) 3968-3972.

48. R.W. Thomas, M.J. Heeg, R.C. Elder, E. Deutsch, *Inorg. Chem.* **24** (1985) 1472-74. "Structural (EXAFS) and solution equilibrium studies on the oxotechntium(V) complexes $TcOX_4^-$ and $TcOX_5^{2-}$ (X = Cl, Br)"

49. M.J. Clarke, M.E. Kastner, M.J. Lindsay, *Inorganic Chemistry* **21** (1982) 2037-2040. "Synthesis Structure and Chemistry of *trans*-$[O_2(en)_2Tc(V)]^+$".

50. S.A. Zuckman, G.M. Freeman, D.E. Troutner, W.A. Volkert, R.A. Holmes, D.G. Van derVeer, E.K. Barefield, *Inorg. Chem.*, **20**, (1981) 2386-2389. "Preparation and X-ray Structure of *trans*-Dioxo(1,4,8,11-tetraazacyclotetradecane)technetium(V) Perchlorate Hydrate."

51. P.H. Fackler, M.E. Kastner, M.J. Clarke, E. Deutsch, *Inorganic Chemistry*, **23**, (1984) 4683-4688. "Synthesis and Structural Characterization of *trans*-$[O_2(TBP)_4Tc(V)]^+$ (TBP = 4-**tert**-butylpyridine) and Related Complexes".

52. M.E. Kastner, P.H. Fackler, M.J. Lindsay, M.J. Clarke, *Inorganica Chemica Acta*, **109**, (1985) 35-49. "Synthesis and Structure of *trans*-$[O_2(Im)_4Tc]Cl.2HO$, *trans*-$[O_2(1\text{-}meIm)_4Tc]Cl.3H_2O$ and Related Compounds".

53. J.F. Rowbottom, G. Wilkinson, *J. Chem. Soc., Dalton*, (1972) 826.

54. H.S. Trop, Ph.D. Thesis, Massachusetts Institute of Technology, 1979.

55. H. Sprinz, M. Wahren, *Z. Chem.*, **21**, (1981) 232.

56. L. Kaden, B. Lorenz, K. Schmidt, H. Sprinz, M. Wahren, *Isotopenpraxis*, **17**, (1978) 174. "Nitridokomplexe des Tc(V)".

57. U. Abram, H. Spies, W. Gorner, R. Kirmse, J. Stach, *Inorg. Chimica Acta* **109**, (1985) L9-L11. "Lipophilic Tc Complexes III. Chelate Complexes of Tc(V) Containing the Tc-Nitrido Core."

58. J. Baldas, J. Bonnyman, P.M. Pojer, G.A. Williams, M. Mackay, *J. Chem. Soc., Dalt. Trans.*, (1981) 1798-1801. "Synthesis & Structure of Bis(diethyldithiocarbamato)nitridotechnetium(V): A Tc-N Triple Bond."

59. J. Baldas, J. Bonnyman, G.A. Williams, *J. Chem. Soc., Dalt. Trans.*, (1984) 833.

60. U. Abram; H. Spies; R. Munze; L. Kaden; B. Lorenz, *J. Nucl. Med. All. Sci.*, **29**, (1985) 185-186. "Nitrido complexes of Tc."

61. G.A. Williams, *J. Nucl. Med. All. Sci.*, **29**, (1985), 217. "Structural chemistry of nitrido complexes of Tc."

62. B.V. DePamphilis, A.G. Jones, A. Davison, *Inorg. Chem.*, **22**, (1983) 2292-2297. "Ligand Exchange Reactivity Patterns of Oxotechnetium(V) Complexes".

63. B.V. DePamphilis, Ph.D. Thesis, Massachusetts Inst. Technology, 1982.

64. D.E. Troutner, J. Simon, A.R. Ketring, W. Volkert, R.A. Holmes, *J. Nucl. Med.*, **21**, (1980) 443-448. "Complexing of ^{99m}Tc with cyclam."

65. S.A. Zuckman, G.M. Freeman, D.E. Troutner, W.W. Volkert, R.A. Holmes, D.G. Van derVeer, E.K. Barefield, *Inorg. Chem.*, **20**,

(1981) 2386-2389. "Preparation and X-ray Structure of *trans*-Dioxo(1,4,8,11-tetraazacyclotetradecane)technetium(V) Perchlorate Hydrate."

66. W.A. Volkert, D.E. Troutner, R.A. Holmes, *Int. J. Appl. Radiat. Isot.* **33** (1982) 891.

67. H.S. Trop, A. Davison, G.H. Carey, B.V. DePamphilis, A.G. Jones, M.A. Davis, *J. Inorg. Nucl. Chem.* **41** (1979) 271-272. "Electrochemical Studies on Halide and Pseudo-Halide Complexes of Tc and Re."

68. H.S. Trop, A. Davison, A.G. Jones, M.A. Davis, D.J. Szalda, S.J. Lippard, *Inorg. Chem.*, **19**, (1980) 1105-1110. "Synthesis and Physical Properties of Hexakis(isothiocyanato)technetate(III) and -(IV) Complexes. Structure of the $[(SCN)_6Tc]^{3-}$ Ion."

69. R.W. Hurst, H.R. Heineman, E. Deutsch, *Inorg. Chem.*, **20**, (1981) 3298-3303. "Technetium Electrochemistry. Spectroelectrochemical Studies of Halogen, diars, and diphos Complexes of Tc in Nonaqueous Media."

70. G.A. Mazzocchin, R. Seeber, U. Mazzi, E. Roncari, *Inorg. Chim. Acta*, **29**, (1978) 1-4. "Voltammetric Behaviour of Technetium Complexes with π-Acceptor Ligands in Aprotic Medium. I. Oxidation of $[TcCl_3(PMe_2Ph)_3]$".

71. G.A. Mazzocchin, R. Seeber, U. Mazzi, E. Roncari, *Inorg. Chim.* Acta, **29**, (1978) 5-9. "Voltammetric Behaviour of ^{99}Tc Complexes with π-Acceptor Ligands in Aprotic Medium. II. Reduction of $[Cl_3(PMe_2Ph)_3Tc]$ and $[Cl_4(PMe_2Ph)_2]$"

72. G. Bandoli, D.A. Clemente, U. Mazzi, *J. Chem. Soc., Dalton Trans.* **2**, (1976) 125.

73. U. Mazzi, A. Bismondo, N. Kotsev, D.A. Clemente, *J. Organomet. Chem.*, **135**, (1977) 172-182. "Phosphine Carbonyl-Tc(I) and Tc(III) Complexes".

74. R.C. Elder, R. Whittle, K.A. Glavan, J.F. Johnson, E. Deutsch, *Acta Cryst.*, **B36** (1980) 1662-1665. "*trans*-dichlorobis[o-phenylenebis(dimethylarsine)]Tc(III) Perchlorate and Chloride Salts."

75. K. Libson, B.L. Barnett, E. Deutsch, *Inorg. Chem.*, **22** (1983) 1695-1704. "Synthesis, Characterization and Electrochemical Properties of Tertiary Diphosphine Complexes of Tc: Single-Crystal Structure of the Prototype Complex *trans*-$[Tc(DPPE)_2Br_2]BF_4$"

76. L. Kaden, B. Lorenz, K. Schmidt, H. Sprinz, M.Z. Wahren, *Z. Chem.* **19**, (1979) 305-306. "Darstellung des Technetium-Distickstoff Komplexes Bis[1,2-bisdiphenylphosphinoethan]distickstoff-technetium".

77. M.J. Abrams, A. Davison, R. Faggiani, A.G. Jones, C.J.L. Lock., *Inorg. Chem.*, **23**, (1984) 3284-3288. "Chemistry and Structure of Hexakis(thiourea-S)technetium(III) Trichloride Tetrahydrate, $[Tc(SC(NH_2)_2)_6]Cl_3 \cdot 4H_2O$."

78. H. Spies, U. Abram, E. Uhlemann, E. Ludwig, *Inorg. Chim. Acta* **109**, (1985) L3-L4. "Synthesis and Characterization of a New Tc Complex: Tris(monothiodibenzoylmethanato)Tc(III)."

79. L.R. Chervu, M.D. Blaufox, *Sem. Nucl. Med.* **12**, (1982) 224-244. "Renal radiopharmaceuticals - an update."

80. E.L. Kramer, J.J. Sanger, *Urology* **23**, (1984) 468-477. "Radionuclide Scanning-New Applications in Urology."

81. G. Gates, *Am. J. Rad.* **138**, (1982) 565. "Glomerular Filtration Rate: Estimation from Fractional Renal Accumulation of ^{99m}Tc-DTPA."

82. P.V. Harper, K.A. Lathrop, A. Gottschalk, G.M. Hinn, in "Pharmacodynamics of some ^{99m}Tc preparations", Andrews, G.A.; Kniseley, R.M.; Wagner, H.N., eds., USAEC Symp. Ser. G., CONF 65111, Springfield, VA, Nat. Bur. Std., 1966, p. 335. "^{99m}Tc Iron Complex".

83. G. Subramanian, J.G. McAfee, E.G. Bell, *et al. J. Nucl. Med.* **12** (1971) 399. "New ^{99m}Tc-Labeled Radiopharmaceuticals for Renal Imaging."

84. O. Charamaza, M. Budikova, *Nucl. Med.* (Stuttgart) **8**, (1969) 301. "^{99m}Tc-Sn-Complex for Renal Scintigraphy".

85. S.L. Kountz, S.H. Yeh, J. Wood, *Nature* **215**, (1967) 1397. "^{99m}Tc(V) Citrate Complex for Estimation of GFR".

86. R.W. Arnold, G. Subramanian, M.G. McAfee, *et al. J. Nucl. Med.* **16**, (1975) 357. "Comparison of ^{99m}Tc-Complexes for Renal Imaging."

87. R.F. Fleay, *Aust. Radiol.* **12**, (1968) 265. "^{99m}Tc Labeled EDTA for Renal Scanning."

88. W.C. Eckelman, P. Richards, *J. Nucl. Med.* **11**, (1970) 761. "Instant ^{99m}Tc-DTPA"

89. L.R. Chervu, H.B. Lee, Q. Goyal, *et al. J. Nucl. Med.*, **18** (1977) 62. "^{99m}Tc-Cu-DTPA Complex as a Renal Function Agent."

90. W. Hauser, H.L. Atkins, K.G. Nelson, *et al. Radiology* **94**, (1970) 679. "^{99m}Tc-DTPA, A New Radiopharmaceutical for Brain and Kidney Scanning."

91. T.H. Lin, A. Khentigan, H.W. Winchell, *J. Nucl. Med.* **15**, (1974) 34. "^{99m}Tc-Chelate Substitute for Organoradiomercurial Renal Agents".

92. R.G. Robinson, D. Bradshaw, B.A. Rhodes, J.A. Spicer, R.J.Visentin, A.H. Gobuty, *Int. J. Appl. Radiat. Isot.* **28**, (1977) 105. "A rapid one-step kit for routine preparation of basic ^{99m}Tc penicillamine."

93. R.G. Robinson, D. Bradshaw, B.A. Rhodes, J.A. Spicer, A.H. Gobuty, *Int. J. Appl. Radiat. Isot.* **28**, (1977) 919 "A Rapid One-Step Kit for the Routine Preparation of Basic ^{99m}Tc-Penicillamine".

94. N. Vanlic-Razumenic, B. Johannsen, H. Spies, *et al. Int J. Appl. Radiat. Isot.* **30,** (1979) 661. "Complex of Tc(V) with 2,3-dimercaptopropansulfonate (Unithiol): Preparation and Distribution in the Rat."

95. L. Darte, M. Oginski, R.B.R. Persson, *J. Nucl. Med.* **18,** (1979) 26. "^{99m}Tc-Unithiol Complex, A New Radiopharmaceutical for Kidney Scintigraphy".

96. A.R. Fritzberg, W.C. Klingensmith, W.P. Whitney, C.C. Kuni, *J. Nucl. Med.* **22,** (1981) 258-263. "Chemical and Biological Studies of ^{99m}Tc-N,N'-bis(mercaptoacetamido)ethylenediamine: A Potential Replacement for ^{131}I-Iodohippurate".

97. A.G. Jones, A. Davison, *et al., J. Nucl. Med.*, **23,** (1982) 801-809. "Chemical and In Vivo Studies of the Anion oxo[N,N'-ethylenebis(2-mercaptoacetimido)]Technetate(V)."

98. A. Davison, A.G. Jones, C. Orvig, M. Sohn, *Inorg. Chem.*, **20,** (1981) 1629-1632. "A New Class of Oxotechnetium(5+) Chelate Complexes Containing a $TcON_2S_2$ Core".

99. C.E. Costello, J.W. Brodack, A.G. Jones, A. Davison, D.L. Johnson, S. Kasina, A.R. Fritzberg, *J. Nucl. Med.* **24,** (1983) 353-355. "The investigation of radiopharmaceutical components by FABMS: The identification of Tc-HIDA and the epimers of Tc-CO_2DADS.

100. D.L. Johnson, A.R. Fritzberg, B.L. Hawkins, S. Kasina, D. Eshima, *Inorg. Chem.*, **23,** (1984) 4204-4207. "Stereochemical Studies of Technetium Radiopharmaceuticals. 1. Fluxional Racemization of Tc and Re Penicillamine Complexes."

101. K.J. Franklin, H.E. Howard-Lock, C.J.L. Lock., *Inorg. Chem.*, **21** (1982) 1941-1946. "Preparation, Spectroscopic Properties and Structure of 1-Oxo-2,3,6-(D-penicillaminato-N,S,O)-4,5-(D-penicillaminato-N,S)Tc(V)".

102. K. Horiuchi, A. Yokoyama, K. Tsuiki, H. Tanaka, H. Saji, *Int. J. Appl. Radiat. Isot.*, **32,** (1981) 545-551. "Effect of the nature of technetium coordination complex on cell membrane permeability: mononuclear complex of ^{99m}Tc-penicillamine ethyl ester."

103. H.B. Bürgi, G. Anderegg, P. Blauenstein, *Inorg. Chem.*, **20,** (1981) 3829-3834. "Preparation, Characterization, and Crystal, Molecular, and Electronic Structure of $[(H_2EDTA)Tc(IV)(\mu\text{-}O)_2Tc(IV)(H_2EDTA)].5H_2O$. A 2.33 A Tc-Tc Distance Which May Represent a $\sigma^2\pi^2\delta^2$ Bond."

104. K.E. Linder, A. Davison, A.G. Jones, *J. Nucl. Med. All. Sci.*, **29,** (1985), 202-203. "An improved synthesis of $[(H_2EDTA)Tc(IV)(\mu\text{-}O)_2Tc(IV)(H_2EDTA)]$."

105. G. Anderegg, E. Muller, K. Zollinger, H.B. Burgi, *Helv. Chim. Acta*, **66,** (1983) 1593-1598. "Preparation, Characterization, Crystal & Molecular Structure Determination of $Na_2[N(CH_2COO)_3Tc^{IV}(\mu\text{-}O)_2Tc^{IV}N(CH_2COO)_3].6H_2O$."

106. B. Noll, S. Seifert, R. Münze, *Radiochem. Radioanal. Lett.*,

43, (1980) 215-218. "New Tc(IV) Compounds with Nitrilotriacetic Acid."

107. E. Deutsch and A. Packard, unpublished results.

108. B. Noll, S. Seifert, R. Münze, *Int. J. Appl. Radiat. Isot.*, **1983**, **34**, 581-584. "Preparation and Characterization of Tc(IV)-Complexes with Diethylenetriaminepentaacetic Acid and Ethylenediaminetetraacetic Acid as Ligands".

109. V.I. Levin, M.A. Gracheva, O.N. Ilyushchenko, *Int. J. Appl. Radiat. Isot.*, **31**, (1980) 382-385. "The stability constant of ^{99m}Tc-DTPA complex."

110. D. Brenner, A. Davison, J. Lister-James, A.G. Jones, *Inorg. Chem.*, **23** (1884) 3793-3797. "Synthesis and Characterization of a Series of Isomeric Oxotechnetium(V) Diamido Dithiolates."

111. A.R. Fritzberg, S. Kasina, D. L. Johnson, D. Eshima, *J. Nucl. Med.*, **26**, (1985), P19. "Triamide mercaptide (N_3S) ligands for ^{99m}Tc as potential ^{99m}Tc renal funotion agents."

112. B.A. Kogen, R. Kay, R.J. Wasnick, H. Carty, *Urology* **21**, (1983) 641. "^{99m}Tc-DMSA Scanning to Diagnose Pyelonephritic Scarring in Children."

113. W. de Kieviet, . *J. Nucl. Med.*, **22**, (1981) 703-709. "Technetium radiopharmaceuticals: Chemical characterization and tissue distribution of Tc-glucoheptonate using ^{99m}Tc and carrier ^{99}Tc."

114. H. Spies, B. Johannsen, *Inorg. Chim. Acta*, **48**, (1981) 255-258. "Oxotechnetium(V)bis(dithiolato) Complexes"

115. H. Spies, B. Johannsen, R. Münze, *Z. Chem.*, **20** (1980) 222-223. "Zur Darstellung von Bis(1,2-dithiolato)oxotechnetat(V) Komplexen."

116. H. Spies, B. Johannsen, *Inorg. Chim. Acta*, **33**, (1979) L113. "Preparation and Characterization of Tetraethylammonium Bis(1,2-dicyanoethylenedithiolato)oxotechnetate(V)."

117. J.E. Smith, E.F. Byrne, F.A. Cotton, *J. Am. Chem. Soc.* **100**, (1978) 5571.

118. L.G. Marzilli, P. Worley, H.D. Burns, *J. Nucl. Med.*, **20**, (1979) 871-876. "A new electrophoretic method for determining ligand:technetium stoichiometry in carrier-free ^{99m}Tc-radiopharmaceuticals."

119. G. Subramanian, J.G. McAfee; *Radiology* **98** (1971) 192. "A New Complex of ^{99m}Tc for Skeletal Imaging."

120. G. Subramanian, J.J. McAfee, O'Mara, R.E.; *et al.*, *J. Nucl. Med.* **12**, (1971) 399. "^{99m}Tc-polyphosphate: A New Radiopharmaceutical for Skeletal imaging."

121. G. Subramanian, J.J. McAfee, E.G. Bell, *et al.*, *Radiology*, **102** (1972) 701. "^{99m}Tc-Labeled Polyphosphate as a Skeletal Imaging Agent."

122. M.A. Davis, Jones, A.L.; *Semin. Nucl. Med.* **6**, (1976) 19. "Comparison of Tc-labeled phosphate and phosphonate for skeletal imaging."

123. R. Perez, Y. Cohen, R. Henry, *et al.*, *J. Nucl. Med.* **13**, (1972) 788. "A new radiopharmaceutical for ^{99m}Tc bone scanning."

124. Y. Yano, J. McRae, D.C. Van Dyke, *et al.*, *J. Nucl. Med.* **16**, (1973) 744. "^{99m}Tc-labeled stannous ethane-1-hydroxy-1,1-diphosphonate: a new bone scanning agent."

125. G. Subramanian, J.J. McAfee, R.J. Blair, *et al.*, *J. Nucl. Med.* **16**, (1977) 1137. "^{99m}Tc-labeled stannous imidodiphosphate, a new radioscintigraphic agent for bone scanning: comparison with other ^{99m}Tc complexes."

126. G. Subramanian, J.J. McAfee, R. Blair, *J. Nucl. Med.*, **16**, (1977) 744. "^{99m}Tc-Methylenediphosphonate: A superior agent for skeletal imaging. Comparison with other Tc complexes."

127. J.A. Bevan, A.J. Tofe, J.J. Benedict, *et al.*, *J. Nucl. Med.* **21**, (1980) 961-966. "^{99m}Tc HMDP (hydroxymethylene diphosphonate): a radiopharmaceutical for skeletal and acute myocardial infarct imaging. I. Synthesis and distribution in animals." *J. Nucl. Med.* **1980, 21**, 967. "II. Comparison of ^{99m}Tc HMDP with other technetium-labeled bone imaging agents in a canine model."

128. J.A.G. Van den Brand, H.A. Das, B.G. Dekker, B.G. *et al.*, *Int. J. Appl. Radiat. Isot.* **30**, (1979) 185. "The influence of experimental conditions on the efficiency of the labeling of 1-hydroxy-ethylidene-1,1-disodium phosphophonate with ^{99m}Tc, using Sn(II) as the reductant."

129. M.D. Harbert, F.H. George, M.L. Kerner, *Clin. Nucl. Med.*, **6**, (1981) 359-361. "Differentiation of rib fractures from metastases by bone scanning."

130. M.D. Bassett, R.H. Gold, M.M. Webber, *Radiol. Clin. N. Am.*, **19**, (1981) 675-701. "Radionuclide Bone Imaging".

131. P.E. Weiss, J.C. Mall, P.B. Hoffer, *et al.*, *Intl. J. Nucl. Med. Biol.*, **4**, (1977) 167. "Radionuclide patterns of femoral head disease."

132. D.O. Dusynski, J.P. Kuhn, E. Afshani, *et al.*, *Radiology*, **117**, (1975) 337. "Early radionuclide diagnosis of acute osteomyelitis."

133. D.R. Brill, *Semin. Nucl. Med.* **11**, (1981) 277-288. "Radionuclide imaging of non-neoplastic soft tissue disorders."

134. M.D. Francis, D.L. Ferguson, A.J. Tofe, J. Bevan, S.E. Michaels, J. Nucl. Med. **21**, (1980) 1185.

135. S. Jurisson, J. Benedict, R.C. Elder, E. Deutsch, R. Whittle, *Inorg. Chem.*, **22**, (1983) 1332. "Calcium affinity of Coordinated Diphosphonate Ligands. Single Crystal Structure

of $[(en)_2Co(O_2P(OH)CH_2P(OH)O_2]Cl_{O4}.H_2O$. Implications for the Chemistry of ^{99m}Tc diphosphonate Skeletal Imaging Agents."

136. K. Libson, E. Deutsch, B.L. Barnett, *J. Am. Chem. Soc* **102**, (1980) 2478-2480. "Structural Characterization of a ^{99}Tc-Diphosphonate Complex. Implications for the Chemistry of ^{99m}Tc Skeletal Imaging Agents."

137. E. Deutsch, B.L. Barnett, "Inorganic Chemistry in Biology and Medicine", A.E. Martell, ed., Am. Chem. Soc. Symp. Ser. #140, Washington, D.C., **1980**, 103-119. "Synthetic and structural aspects of technetium chemistry as related to nuclear medicine."

138. S.C. Srivastava, D. Bandyopadhyay, G. Meinken, G.; P. Richards, *J. Nucl. Med.* **22**, (1981) 69 (abstr.). "Characterization of ^{99m}Tc-bone agents (MDP, HEDP) by reverse phase and ion exchange HPLC."

139. T.C. Pinkerton, W.R. Heineman, E. Deutsch, *Anal. Chem.* **52**, (1980) 1106-1110. "Separation of Technetium hydroxyethylidene diphosphonate complexes by anion-exchange HPLC."

140. T.C. Pinkerton, Ferguson, D.L.; E. Deutsch, W.R. Heineman, Libson, K., *Int. J. Appl. Radiat. Isot.* **1982, 33**, 907.

141. S.C. Srivastava, Meinken, G.E.; Richards, P. in "Abstracts of the Third World Congress of Nucl. Med. and Biol." Paris, 1982. "HPLC Characterization of Clinically used ^{99m}Tc Bone Agents. Relative Tissue Distribution of Fractionated Components in Mice.

142. L.R. Chervu, A.D. Nunn, M.D. Loberg, *Sem. Nucl. Med.* **12**, (1982) 5-17. "Radiopharmaceuticals for Hepatobiliary Imaging."

143. D.E. Drum, *Sem. Nucl. Med.* **12**, (1982) 64-74. "Current status of radiocolloid hepatic scintophotography for space-occupying disease."

144. M.A. Tempero, R.J. Petersen, R.K. Zetterman, H.M. Lemon, M.D. Gurney, *J. Am. Med. Assoc.*, **248**, (1982) 1329-1332. "Detection of metastatic liver disease."

145. M. Christensen, P.M. Jakobsen, P. Johansen, *Acta Chir. Scand.*, **147**, (1981) 269-270. "The value of liver scintigraphy in the management of patients with suspected gastric cancer."

146. W.D. Kaplan, W.D. Ensminger, *et al.*, *Canc. Treat. Rep.* **64**, (1980) 1217-1222. "Radionuclide angiography to predict patient response to hepatic artery chemotherapy."

147. H.S. Weissmann, K.J.C. Byun, L.M. Freeman, *Sem. Nucl. Med.* **13**, (1983) 199-222. "Role of ^{99m}Tc IDA Scintrigraphy in the Evaluation of Hepatobiliary Trauma."

148. M.D. Loberg, M. Cooper, E. Harvey, P. Callery, and W. Faith, *J. Nucl. Med.* **17**, (1976) 633. "Development of new

radiopharmaceuticals based on N-substitution of iminodiacetic acid."

149. M.D. Loberg, A.T. Fields, *Int. J. Appl. Radiat. Isotop.* **19,** (1978) 167. "Chemical structure of the ^{99m}Tc-labeled N(2,6-dimethyl-carbamoylmethyl) iminodiacetic acid (Tc-HIDA)."

150. R.J. Baker, J.C. Bellen, *Int. J. Nucl. Med. Biol.* **4,** (1977) 85. "^{99m}Tc biliary scanning agents based on pyridoxal: effect of the amino acid component on labeling and biological distribution."

151. E. Chiotellis, G. Subramanian, J.G. McAfee, *Int. J. Nucl.* Med. Biol. **4,** (1977) 29-41. "Preparation of ^{99m}Tc labeled pyridoxal amino acid complexes and their evaluation."

152. M. Kato, M. Hazue, *J. Nucl. Med.* **19,** (1978) 397-406. "^{99m}Tc (Sn) pyrdioxilidene aminates: Preparation and biological evaluation."

153. M. Kato-Azuma; *Int. J. Appl. Radiat. Isot.*, **32,** (1981) 187-189. "Identification of a mixed-ligand complex of ^{99m}Tc: a chromatographic approach to the chemical structure of carrier free ^{99m}Tc(Sn)pyridoxylideneaminate."

154. G. Bandoli, U. Mazzi, D.A. Clemente, E. Roncari, *J. Chem. Soc., Dalt. Trans.*, (1982) 2455-2459. "Synthesis of a Six-coordinate Tc(V) Complexes with N-Phenylsalicylideneimine. X-ray Crystal Structure of Chloro-oxobis(N-Phenylsalicylideneimine)technetium(V)."

155. M. Kato-Azuma, M. Hazue, in "Abstracts of the Third Intl. Symp. on Radiopharm. Chem.", Welch, M.J., ed., Washington Univ., St. Louis, 1980." "Preparation and biological evaluation of lipophilic derivatives of ^{99m}Tc(Sn) pyrilidoxylidenephenylalanine: an approach to structure/bio-distribution relationships of technetium complexes."

156. E. Harvey, M.D. Loberg, M. Cooper, *J. Nucl. Med.* **16,** (1975) 533. "A new radiopharmaceutical for hepatobiliary imaging."

157. L.G. Marzilli, R.F. Dannals, Burns, H.D. in "Inorganic Chemistry in Biology and Medicine", A.E. Martell, ed., Am. Chem. Soc. Symp. Ser. #140, Washington, D.C., **1980,** 93-101. "^{99m}Tc-Radiopharmaceuticals."

158. A.T. Fields, D.W. Porter, P.S. Callery, *et al. J. Label. Comp. Radiopharm.* **15,** (1978) 387-399. "Synthesis and radiolabeling of Tc radiopharmaceuticals based on N-substituted iminodiacetic acid: Effect of radiolabeling conditions on radiochemical purity.

159. D. Burns, L. Marzilli, D. Sowa, *J. Nucl. Med.***18,** (1977) 624. "Relationship between molecular structure and biliary excretion of ^{99m}Tc HIDA and HIDA analogs."

160. M.A. Rothschild, M. Oratz, S.S. Schreiber, *Sem. Liver Disease*, **2,** (1982) 29-40. "Comments on radionuclide hepatic scanning."

161. M.D. Loberg, Porter, D.W., in "Radiopharmaceuticals II",

Sorenson, J.A., ed., Proc. 2nd Intl. Symp. Radiopharm., Soc. Nucl. Med., New York, 1979, 519-544. "Review and current status of hepatobiliary agents."

162. A.R. Fritzberg, D. Lewis, *J. Nucl. Med.* **21**, (1980) 1180. "HPLC analysis of ^{99m}Tc Iminodiacetate hepatobiliary agents and a question of multiple peaks."

163. N.N. Greenwood, A. Earnshaw, "Chemistry of the Elements", Pergamon Press, New York, **1984**, 255.

164. G.M. Pohost, K.A. McKusick, H.W. Strauss, in "Radiopharmaceuticals II", Sorenson, J.A., ed., Soc. Nucl. Med., New York, 1979, 465-473. "Physiologic basis and utility of myocardial perfusion imaging."

165. E. Deutsch, W. Bushong, K.A. Glavan, R.C. Elder, V.J. Sodd, K.L. Scholz, D.L. Fortman, S.J. Lukes, *Science* **1981**, 85. "Heart Imaging with Cationic Complexes of Tc."

166. E. Deutsch, K.A. Glavan, V.J. Sodd, H. Nishiyama, D.L. Ferguson, J.J. Lukes, *J. Nucl. Med.* **22**, (1981) 897-907. "Cationic ^{99m}Tc complexes as potential myocardial imaging agents."

167. H. Nishiyama, E. Deutsch, R.J. Adolph, V.J. Sodd, *et al*, *J. Nucl. Med.* **23**, (1982) 1093. "Basal kinetic studies of ^{99m}Tc-DMPE as a myocardial imaging agent in the dog."

168. H. Nishiyama, R.J. Adolph, E. Deutsch, V.J. Sodd, *et al. J. Nucl. Med.* **23**, (1982) 1102. "Effect of coronary blood flow on uptake and washout of ^{99m}Tc-DMPE and ^{201}Tl."

169. E. Deutsch, K.A. Glavan, W. Bushong, V.J. Sodd, *J. Appl. Nucl. Radiochem.* **1982**, 139. "The inorganic chemistry of ^{99m}Tc myocardial imaging agents."

170. J.L. Vanderheyden, K. Libson, D.L. Nosco, A.R. Ketring, E. Deutsch, *Int. J. Appl. Radiat. Isot.* **34**, (1983) 1611. "Preparation & Characterization of $[^{99m}Tc(DMPE)_2X_2]^+$, X = Cl, Br (DMPE = 1,2-bisdimethylphosphinoethante)."

171. M.C. Gerson, E.A. Deutsch, *et al. Eur. J. Nucl. Med.* **8**, (1983) 371. "Myocardial perfusion imaging with ^{99m}Tc-DMPE in man."

172. M.C. Gerson, E.A. Deutsch, *et al. Eur. J. Nucl. Med.* **9**, (1984) 403. "Myocardial scintigraphy with ^{99m}Tc-DMPE in man."

173. J. Vanderheyden, A.R. Ketring, K. Libson, M.J. Heeg, L. Roecker, P. Motz, R. Whittle, R.C. Elder, E. Deutsch, *Inorg. Chem.*, **23**, (1984) 3184-3191. "Synthesis and Characterization of Cationic Technetium Complexes of 1,2-Bis(dimethylphospino)ethane (DMPE). Structure Determinations of *trans*-$[O(OH)(DMPE)_2Tc^{V}](F_3CSO_3)_2$, *trans*-$[Cl_2(DMPE)_2Tc^{III}]F_3CSO_3$ and *trans*-$[(DMPE)_3Tc^{I}]^+$ Using X-ray Diffraction, EXAFS and ^{99}Tc NMR."

174. J.E. Fergusson, R.S. Nyholm, *Nature* **183**, (1959) 1039.

175. J.L. Vanderheyden, M.J. Heeg, E. Deutsch, *Inorg. Chem.* **24**, (1985) 1666-1673. "Comparison of the chemical and biological properties of $[Cl_2(DMPE)_2Tc]^+$ and $[Cl_2(DMPE)_2Re]^+$, where DMPE = 1,2-bis(dimethylphosphino)ethane. Single crystal structural analysis of *trans*-$[Cl_2(DMPE)_2Re]PF_6$"

176. M.J. Abrams, A. Davison, A.G. Jones, C.E. Costello, *Inorg. Chem.* **22** (1983) 2798-2800. "Synthesis and characterization of hexakis(alkyl isocyanide) and hexakis(aryl isocyanide) complexes of Tc(I)."
A.G. Jones, J.F. Kronauge, A. Davison, *J. Nucl. Med. Allied Sci.* **29** (1985) 200. "Biological distribution and structure-function relationships of hexakis(isonitrile)-Tc(I) complexes."
K.E. Linder, A. Davison, A.G. Jones, *J. Nucl. Med. Allied Sci.* **29** (1985) 203. "Attempted oxidations of $[Tc(CNR)_6]^+$; preparation of $[Tc(II)(CNR)_6]^{2+}$ and $[Tc(I)(CNR)_5(NO)]^{2+}$."]

177. F.J. Bonte, R.W. Parkey, K.D. Graham, *et al. Radiology* **110**, (1974) 473. "A new method for radionuclide imaging of myocardial infarcts."

178. S. Bloom, D.L. Davis, *Am. J. Pathol.* **69** (1972) 459. "Calcium as a mediator of isoproterenol-induced myocardial necrosis."

179. H.F. Kung, M. Blau, R. Ackerhalt, in "Radiopharmaceuticals II", Sorenson, J.A., ed., Soc. Nucl. Med., New York, 1979, 475-485. "Uptake of radiopharmaceuticals in developing myocardial lesions."

180. A. Singh, M. Usher, *J. Nucl. Med.* **18**, (1977) 790. "Comparison of ^{99m}Tc methylene diphosphonate with ^{99m}Tc pyrophosphate in the detection of acute myocardial infarction."

181. J.G. Jacobstein, D.R. Alonso, A.J. Roberts, *et al. J. Nucl. Med.* **18**, (1977) 413. "Early diagnosis of myocardial infarct in dog with ^{99m}Tc-glucoheptonate."

182. S.C. Srivastava, L.R. Chervu, *Sem. Nucl. Med.* **14**, (1984) 68-82. "Radionuclide-Labeled Red Blood Cells: Current status and future prospects."

183. K.D. Schwartz, M. Kruger, *J. Nucl. Med.* **12**, (1971) 323-324. "Improvement in labeling erythrocytes with ^{99m}Tc pertechnetate."

184. M.M. Rehani, S.K. Sharma, *J. Nucl. Med.* **21**, (1980) 676. "Site of ^{99m}Tc binding to the red blood cell."

185. M.K. Dewangee, *J. Nucl. Med.* **15**, (1974) 703-706. "Binding of ^{99m}Tc to hemolgobin."

186. T.D. Smith, P. Richards, *J. Nucl. Med.* **17**, (1976) 126. "A simple kit for the preparation of ^{99m}Tc-labeled red blood cells."

187. S.C. Srivastava, D. Babich, P. Richards, *J. Nucl. Med.* **24**, (1983) 128. "A new method for the selective labeling of erythrocytes in whole blood with ^{99m}Tc."

188. Pyrophosphate is substituted for citrate and the amount of Sn(II) used is ~15 μg per kg body weight.

189. M.W. Billinghurst, D. Jette, D. Greenburg, *Int. J. Appl. Radiat. Isot.* **31**, (1980) 499. "Determination of the optimal concentrations of stannous pyrophosphate for *in vivo* red blood cell labeling with ^{99m}Tc."

190. R.J. Callahan, J.W. Froelich, K.A. McKusick, *et al. J. Nucl. Med.* **23**, (1982) 315. "A modified method for the *in vivo* labeling of red blood cells with ^{99m}Tc."

191. W.H. Strauss, K.A. McKusick; C.A. Boucher, *et al. Sem. Nucl. Med.* **9**, (1979) 296-309. "Of linen and laces: the eighth anniversary of the gated blood pool scan."

192. G.C. Winzelberg, K.A. McKusick, J.W. Froelich, *et al Sem. Nucl. Med.* **12**, (1982) 139-146. "Detection of gastrointestinal bleeding with ^{99m}Tc-labeled red blood cells."

193. D. Front, O. Israel, D. Grosher, J. Weininger, *Sem. Nucl. Med.* **14**, (1984) 226-250. "^{99m}Tc Labeled Red Blood Cell Imaging."

194. J.G. McAfee, G. Subramanian, G. Gagne, *Sem. Nucl. Med.*, **14**, (1984) 83-106. "Technique of leukocyte harvesting and labeling: problems and perspectives."

195. M.K. Dewanjee, *Sem. Nucl. Med.*, **14**, (1984) 154-187. "Cardiac and vascular imaging with labeled platelets and leukocytes."

196. G.R. Spencer, C. Bird, D.L. Prothero, *et al* ^{99m}*Brit. J. Surg.*, **68**, (1981) 412-413. "Spleen scanning with ^{99m}Tc-labeled red blood cells after splenectomy.

197. C.P. Ehrlich, N. Papanicalau, S. Treves, *et al.*, *J. Nucl.* ^{99m}Tc Med. **23**, (1982) 209-213. "Splenic scintigraphy using ^{99m}Tc-labeled heat-damaged red blood cells in pediatric patients."

198. S.M. Larson, W.B. Nelp, *J. Nucl. Med.* **7**, (1966) 817. "Radiopharmacology of a simplified ^{99m}Tc-colloid preparation for photoscanning."

199. D.L. Fortman, in "Radiopharmaceuticals II" ^{99m}J.A. Sorenson, ed., Soc. Nucl. Med., NY, 1979, 15-23. "^{99m}Tc-Sulfur Colloid - Evaluation parameters for kits from four commercial manufacturers."

200. M.A. Davis, A.G. Jones, H. Trindade, *J. Nucl. Med.*, **15**, (1974) 923. "A rapid and accurate method for sizing radiocolloids."

201. M. Frier, P. Griffiths, A. Ramsay, *Eur. J. Nucl. Med.* **6**, (1981) 255-260. "The physical and chemical characteristics of sulfur colloids."

202. R. Taillefer, G. Beauchamp, *Clin. Nucl. Med.*, **9**, (1984) 465-483.

203. W.D. Bloomer, *Sem. Nucl. Med.*, **13**, (1983) 54-60. "Lymphoscintigraphy in gynecological malignancies."

204. O.L. Garzon, M.C. Palcos, R.A. Radicella, *Int. J. Appl.* Radiat. Isot., **16**, (1965) 613. "A ^{99m}Tc labeled colloid."

205. A. Warbick, G.N. Ege, R. M. Henkelman, G. Maier, D.M. Lyster, *J. Nucl. Med.* , **18**, (1977) 827-834. "An evaluation of radiocolloid particle sizing techniques."

206. B.M. Gallagher, M.L. Delano, R. Watt, *et al.*, *J. Nucl. Med.*, **21**, (1980) 36. "A comparison of radiopharmaceuticals for lymphoscintigraphy."

207. L. Bergquist, S.E. Strand, B.R. Persson, *Sem. Nucl. Med.*, **13**, (1983) 9-19. "Particle sizing and biokinetics of interstitial lymphoscintigraphic agents."

208. W. Kaplan, *Sem. Nucl. Med.*, **13**, (1983) 42-53. "Iliopelvic lymphoscintigraphy."

209. G.N. Ege, *Sem. Nucl. Med.*, **13**, (1983) 16-34. "Lymphoscintigraphy-techniques and applications in the management of breast carcinoma."

210. R.W. McConnell, B.G. McConnell, E.E. Kim, *Sem. Nucl. Med.*, **1983, 13**, 70-74. "Other applications of interstitial lymphoscintigraphy."

211. M. Villa, O. Pretti, G. Plassio, *Int. J. Nucl. Med. Biol.*, **5**, (1978) 51. "Preparation and labeling of tin-albumin microspheres by a single-step procedure."

212. D.M. Lyster, J.R. Scot, *et al.*, *J. Nucl. Med.*, **15**, (1974) 198. "Preparation of a ^{99m}Tc-MAA kit for use in nuclear medicine."

213. M.A. Davis, *J. Nucl. Med.*, **12**, (1971) 349. "Long-term iron retention in lungs perfused with iron hydroxide aggregates."

214. R.J. Lull, J.L. Tatum, H.J. Sugerman, M.F. Hartshorne, D.A. Boll, K.A. Kaplan, *Sem. Nucl. Med.*, **13**, (1983) 223-237. "Radionuclide evaluation of lung trauma."

215. F.H. DeLand, *J. Nucl. Med.* **19**, (1978) 858. "Plasma volume determination after 20 years."

216. W.A. Pettit, F.H. DeLand, S.J. Bennett, *J. Nucl. Med.*, **21** (1980) 59. "Improved protein labeling by stannous tartrate reduction of pertechnetate."

217. W.A. Pettit, F.H. DeLand, G.H. Pepper, *et al. J. Nucl. Med.* **19**, (1978) 387. Characterization of tin-technetium colloid in technetium albumin preparations."

218. J. Steigman, H.P. Williams, N.A. Solomon, *J. Nucl. Med.* **16**, (1975) 573. "The importance of the protein sulfhydryl group in HSA labeling with ^{99m}Tc."

219. J. Korteland, B.G. Dekker, C.L. DeLigny, *Int. J. Appl* Radiat. Isot. **31**, (1980) 315. "The valence state of ^{99m}Tc in its complexes with bleomycin, 1-hydroxy-ethylidene-1,1-diphosphonate and human serum albumin."

220. G. Meinken, S.C. Srivastava, T.D. Smith, *et al. J. Nucl. Med.* **17**, (1975) 537. "Is there a good ^{99m}Tc-albumin?"

221. A. Davison, R.M. Perlstein, P.A. Mabrouk, A.G. Jones, M.M. Morelock, *J. Nucl. Med. All. Sci.*, **19**, (1985), 194. "Resonance Raman studies on Tc complexes."

222. J.F. Harwig, S.S.L. Harwig, *et al. Int. J. Appl. Radiat. Isot.* **27**, (1976) 5. "Preparation and *in vitro* properties of ^{99m}Tc fibrinogen."

223. W.T. Millar, J.F.B. Smith, *Lancet* (1974) 695. "Localization of deep-venous thrombosis using radioactive urokinase."

224. J.J. Kozar, H.S. Stern, *J. Nucl. Med.*, **14**, (1973) 629. "^{99m}Tc-streptokinase: improved labeling efficienoy and purification."

225. E.B. Silberstein, *Sem. Nucl. Med.*, **13**, (1983) 153-167. "Brain scintigraphy in the diagnosis of the sequelae of head trauma."

226. M.D. Loberg, E.H. Corder, A.T. Fields, P.S. Callery, *J. Nucl. Med.*, **20**, (1979) 1181-1188. "Membrane transport of ^{99m}Tc-labeled radiopharmaceuticals. I. Brain uptake by passive transport."

227. S. Jurisson, E. Schlemper, D.E. Troutner, L.R. Canning, D.P. Nowotnik, *J. Nucl. Med. All. Sci.*, **29**, (1985), 201. "Synthesis, characterization and x-ray structural determinations of neutral Tc(V) oxo tetradentate amine oxime complexes."

228. D.P. Nowotnik, L.R. Canning, *et al.*, *J. Nucl. Med. All. Sci.*, **29**, (1985), 209. "^{99m}Tc-HM-PAO: A new radiopharmaceutical for imaging regional cerebral blood flow."

229. C. Palm, E.O. Fischer, *Tetr. Lett.*, (1962) 253-254. "Di-Benzol-Technetium(I) Kation in Wagbaren Mengen Uber Aromatenkomplexe von Metallen - LX."

230. R.T. Dean, D.W. Wester, (1985) to be submitted for publication.

231. M. Iturralde, P.F. Venter, *Sem. Nucl. Med.* **11**, (1981) 301-314. "Hysterosalpingo-radionuclide scintigraphy (HERS)."

232. L.E. Holder, J.R. Martire, H.K.A. Schirmer, *J. Am. Med. Soc.*, **245**, (1981) 2526-2529. "Clinical applications of testicular radionuclide angiography and scrotal scanning."

233. J.E. Freitas, M.D. Gross, S. Ripley, B. Shapiro, *Sem. Nucl. Med.*, **15**, (1985) 106-130. "Radionuclide diagnosis and therapy of thyroid cancer: current status report."

234. G.G. Winzelberg, J.D. Hydovitz, *Sem. Nucl. Med.*, **15**, (1985) 161-170. "Radionuclide imaging of parathyroid tumors: historical perspectives and newer techniques."

235. H.S. Winchell, *Sem. Nucl. Med.*, **6**, (1976) 371. "Mechanisms for localization of radiopharmaceuticals in neoplasms."

236. V.R. McCready, *Br. Med. Bull.*, **36**, (1980) 209-213. "Tumor localization."

237. P.J. Ell, O. Khan, *Sem. Nucl. Med.*, **11**, (1981) 50-60. "Emission computerized tomography: clinical applications."

238. C.M. Mansfield, C.H. Park, *Sem. Nucl. Med.*, **15**, (1985) 28-45.

239. D.L. Citrin, D.C. Tormey, P.P. Carbone, *Canc. Treat. Rep.*, **61**, (1977) 1249-1251. "Implications of the ^{99m}Tc-diphosphonate bone scan on treatment of primary breast cancer."

240. R.V. Smalley, L.S. Malmud, W.G.M. Ritche, *Seminars in Oncology*, **7**, (1980) 358-369. "Preoperative scanning: evaluation for metastatic disease in carcinoma of the breast, lung, colon, bladder and prostate."

241. F.S. Chew, T.M. Hudson, W.F. Enneking, *Sem. Nucl. Med.*, **11**, (1981) 266-275. "Radionuclide imaging of soft tissue neoplasms."

242. P. Martin-Simmerman, M.D. Cohen, A. Sidiqui, D. Mirkin, A. Provisor, *J. Nucl. Med.*, **25**, (1984) 656-660. "Calcification and Uptake of ^{99m}Tc Diphosphonates in Neuroblastoma."

243. L.R. Bennett, G. Lago, *Sem. Nucl. Med.*, **13**, (1983) 61-69. "Cutaneous lymphoscintigraphy in malignant melanoma."

244. J.G. Van Weelde, E.K.J. Pauwels, A.T. Van Oosterom, *Clinical Radiology*, **35**, (1984) 465-468. "Scintigraphic Peritoneography in Advanced Ovarian Malignancies: Its Value for Chemotherapeutic Distribution Studies."

245. E. Cancroft, C.R. Goldfarb, *Sem. Nucl. Med.*, **11**, (1981) 289. "Breast scintigraphy as an imaging modality in the diagnosis of breast masses."

246. D.W. Wong, A. Mandal, I.C. Reese, J. Brown, R. Siegler, ***Int. J. Nucl. Med. Biol., 10, (1983) 211-218. "In Vivo Assesment of ^{99m}Tc-Labeled Hematoporphyrin Derivative in Tumor-Bearing Animals."***

247. D.R. Elmaleh, P.C. Zamecnik, F.P. Castronovo, H.W. Strauss, E. Rapaport, Proc. Natl. Acad. Sci., USA. **81**, (1984) 918-921. "^{99m}Tc-Labeled Nucleotides as Tumor-Seeking Radiodiagnostic Agents."

248. N. Murugesan, S.M. Hecht, *J. Am. Chem. Soc.*, **107**, (1985) 493-500. "Bleomycin as an oxene transferase. Catalytic oxygen transfer to olefins."

249. V. Sugiura, *et al.*, *J. Biol. Chem.*, **258**, (1983) 1328-1336. "Synthetic analogues and biosynthetic intermediates of bleomycin."

250. K.A. Krohn, J.M. Meyers, G.L. DeNardo, S.J. Denardo, *J. Nucl. Med.*, **18**, (1977) 276-281. "Comparison of radiolabeled bleomycins and gallium ctirate in tumor-bearing mice."

251. M.D. Silberstein, *Am. J. Med.*, **60**, (1976) 232-236. "Cancer diagnosis: the role of tumor-imaging radiopharmaceuticals."

252. T. Gerber, *J. Nucl. Med. All. Sci.*, **29**, (1985), 198. "Interaction of the antibiotic lasalocid A with Tc(V) in methanol."

253. E. Sundrehagen, *Eur. J. Nucl. Med.*, **8**, (1983) 447-49. "Radiochemical quality control of ^{99m}Tc-labelled immunoglobin G by immobilised protein A from S. aureus."

254. S.M. Larson, J.A. Carrasquillo, M.D. Reynolds, *Cancer Investigation*, 2, (1984) 363-381. "Radioimmunodetection and radioimmunotherapy."

255. E.K.J. Pauwels, F.J. Cleton, *Radiotherapy and Oncology*, **1**, (1984) 333-338. "Radiolabelled monoclonal antibodies: a new diagnostic tool in nuclear medicine."

256. N. Javadpour, E.E. Kim, F.H. Deland, J.R. Salyer, U. Shah, D.M. Goldenberg, *J. Am. Med. Assoc.*, **246**, (1981) 45-49. "The role of radioimmunodetection in the management of testicular cancer."

257. L. Callegaro, G. Deleide, E. Cecconato, G.A. Scasselati, *J. Nucl. Med. All. Sci.*, **29**, (1985), 189. "^{99m}Tc-Labelling and acceptance testing of radiolabelled monoclonal antibodies."

258. M.V. Pimm, A.C. Perkins, R.W. Baldwin, *Behring Inst. Mitt.*, **74**, (1984) 61-71. "Immunoscintigraphy of tumors: possibilities and limitations."

259. D.J. Hnatowich, R.L. Childs, D. Lanteigne, A. Najafi, *J. Immunol. Meth.*, **65**, (1983) 147-157. "The preparation of DTPA-coupled antibodies radiolabeled with metallic radionuclides: an improved method."

260. P. Orlando, G. Galli, C. Giordano, G. Valle, *J. Nucl. Med. All. Sci.*, **29**, (1985), 209. "^{99m}Tc-labelled alpha-1-asialoglycoprotein in scintigraphic studies."

261. P. Robertson, R.G. Hiskey, K.A. Kochler, *J. Biol. Chem.*, **253**, (1978) 5880.

262. R.A. Armstrong, H. Taube, *Inorg. Chem.*, **15** (1976) 1904-1909. "Chemistry of *trans*-Aquonitrosyltetraamminetechnetium(I) and Related Studies.

263. L.L. Hwang, N. Ronca, N. Solomon, J. Steigman, *Int. J. Appl. Radiat. Isot.* **36** (1985) 475-480. "Complexes of Tc with polyhydric ligands."